B A S E P R E S S U R E

A T S U P E R S O N I C V E L O C I T I E S

Thesis by

Dean R. Chapman

In Partial Fulfillment of the Requirements

For the Degree of

Doctor of Philosophy

California Institute of Technology

Pasadena, California

1948

ACKNOWLEDGEMENTS

It is a pleasure to express thanks to Dr. H. W. Liepmann for his particularly helpful advice in the writing of this thesis, and for the valuable and always-constructive criticism which he gave during the course of the investigation.

Acknowledgement is also gratefully made of the cooperation of A. C. Charters and the Ballistic Research Laboratories in making available numerous spark shadowgraphs for use in the present study of base pressure. These shadowgraphs, several of which are reproduced herein, have been of much help in understanding the physical phenomenon involved in the problem; they have also been of great value in comparing the theory with some of the available experimental results.

SUMMARY

The existing theories of base pressure are described in detail and are shown to be unsatisfactory. An "exact" analysis is then made of the base pressure in an inviscid fluid, both for two-dimensional and axially-symmetric flow. It is shown that for a given body there are, in general, an infinite number of possible solutions satisfying all necessary boundary conditions. For the particular case of inviscid flow about projectile-shaped bodies only one solution is possible, but it corresponds to zero base drag. This latter result is generalized and the following conjecture made: it is impossible for a steady axially-symmetric inviscid supersonic flow to converge toward, and to meet the axis at a finite (non-zero) angle.

Since the inviscid-fluid theory does not adequately describe the conditions in a real fluid, an approximate theory for base pressure in a viscous fluid is developed. This latter theory is based in part on the inviscid-flow calculations and in part on dimensional analysis. It includes the effects of Mach number, Reynolds number, body shape, and type of boundary-layer flow. A comparison of the theory with the available experimental data indicates satisfactory agreement.

It is shown that under certain conditions the airfoil contour for minimum profile drag in a viscous fluid necessarily has a blunt trailing edge. Approximate calculations indicate that very substantial reductions in profile drag are possible by designing airfoils with blunt trailing edges. Consideration is briefly given to the interference of a support rod on base pressure measurements in a supersonic wind tunnel.

CONTENTS

PART I. INTRODUCTION

The problem investigated herein is concerned with the pressure acting on the base of a body moving at a supersonic velocity. This problem is of considerable practical as well as theoretical importance since in some cases the base drag amounts to as much as two-thirds of the total drag of a body. In the past ten years numerous measurements of base pressure have been made both in supersonic wind tunnels and in free flight. These experimental investigations have had no theory to guide them, and as a result, the present day knowledge of base pressure is very limited.

The existing theories of base pressure are unsatisfactory either for predicting the base pressure or for correlating the various experimental measurements. These theories and their many shortcomings are discussed in detail in part II of this thesis. It is apparent that a completely new theory is needed.

The problem of base pressure in a real fluid is so tremendously complicated that a satisfactory mathematical treatment of the real physical situation is hopeless in the present state of gas dynamics. Accordingly, some simplified approach is necessary. There are two such approaches that can be taken in the present problem. First, the actual physical problem could be idealized and an exact mathematical analysis made of base pressure in an inviscid flow. Second, the actual physical problem could be treated by an approximate mathematical analysis. These two approaches are taken up in detail in parts III and IV, respectively.

Although the central problem of this investigation is of

direct importance to the field of ballistics, it is to be emphasized that the fundamental physical phenomena involved are in principle exactly the same as those encountered in many aerodynamic problems. The base-pressure problem may be thought of as a special case—and probably the simplest case—of the many flow-separation problems occurring in supersonic aerodynamics. The problem of base pressure on a body without boat-tailing is relatively simple compared to other separation problems because the point of separation always remains fixed regardless of the Mach number, Reynolds number, or type of boundary-layer flow. The more general problem involves separation on a curved surface where the point of separation varies with each of the above-mentioned parameters. A satisfactory understanding of these more complex separation phenomena, however, will probably not be reached until the more simple problem of base pressure is well understood.

PART II. EXISTING THEORIES OF BASE PRESSURE

The existing theories of base pressure are necessarily phenomenological in nature. Each theory follows the same general pattern: a model of the mechanism which is assumed to govern the flow is first set up, and then the laws of fluid mechanics are applied to calculate the pressure acting on the base of the body. The success or failure of such theories, therefore, depends almost entirely on the correctness of the assumed flow model on which each theory is based. Since the published literature on the existing theories of base pressure consists of only three papers, two of which are rarely referred to, a complete but brief account of these theories is given in the remainder of this section.

To the author's knowledge the first attempt at formulating a mechanism which governs the supersonic flow over the base of a body of revolution was given by Lorenz (reference 1). He reasoned that due to the supersonic speed of the body there is a tendency for a very low pressure to exist at the base, but that a vacuum could not exist there since the maximum possible velocity with which the air could flow laterally into the space behind the base would be the kinetic velocity of the air molecules. Although Lorenz did not employ this concept any further in order to calculate the base pressure, it is not difficult to do so. The final result is quite interesting even though the concept on which it is based is incorrect.

From the simplified kinetic theory of a perfect gas the mean kinetic velocity, U_{KE}, of the molecules is known to be given by

$$U_{KE}^2 = \frac{8}{\pi} RT = \frac{8}{\pi\gamma} a_b^2$$

where a_b is the velocity of sound of the fluid just outside the dead-air region. Let U_b be the velocity corresponding to a_b, then the pressure p_b corresponding to this velocity would be the same as the base pressure. The energy equation is

$$\frac{a_b^2}{\gamma-1} + \frac{U_b^2}{2} = \frac{a_\infty^2}{\gamma-1} + \frac{U_\infty^2}{2} \qquad (2.1)$$

where U_∞ is the free-stream velocity. Equation (2.1) together with the Pythagorean theorem and the concept of Lorenz gives

$$\frac{U_b^2}{U_\infty^2} = 1 + \frac{U_{KE}^2}{U_\infty^2} = 1 + \frac{8}{(\pi\gamma+4\gamma-4)M_\infty^2}$$

The base pressure coefficient is determined from the velocity by using the well-known relation for isentropic flow

$$P_b = \frac{p_b - p_\infty}{\frac{1}{2}\rho_\infty U_\infty^2} = \frac{2}{\gamma M_\infty^2}\left[\left\{1 + \frac{\gamma-1}{2}M_\infty^2\left(1-\frac{U_b^2}{U_\infty^2}\right)\right\}^{\frac{\gamma}{\gamma-1}} - 1\right] \qquad (2.2)$$

Hence, according to the hypothesis of Lorenz,

$$P_b = \frac{2}{\gamma M_\infty^2}\left[\left\{\frac{\pi\gamma}{(\pi+4)\gamma-4}\right\}^{\frac{\gamma}{\gamma-1}} - 1\right] = -\frac{0.945}{M_\infty^2} \qquad (2.3)$$

This equation is plotted in figure 1. As a basis of comparison for the various theories, approximate experimental values taken at relatively large Reynolds numbers (reference 2) are also shown in this figure. Although Lorenz's concept is certainly not correct, it may be seen from the curves that at Mach numbers greater than about 3 the base pressure calculated from this erroneous concept is accidentally in quite good agreement with the experiments.

The first serious mathematical attempt to develop a complete

theory for the base pressure was given by Gabeaud in 1931 (reference 3). He pictured the flow in the wake as consisting of a series of vortex rings periodically trailing from the base in much the same way as vortex filaments are shed in the two-dimensional Kármán vortex street. By assuming that the drag is equal to the transport of momentum of the vortex rings, and by utilizing an electro-magnetic analogy (of questionable validity), Gabeaud calculated the base pressure coefficient to be

$$P_b = -\frac{K}{4}$$

where

$$K = \tfrac{1}{4}(1+M_\infty^2) \quad \text{for } M_\infty < 1$$
$$K = 1 \quad \text{for } M_\infty > 1 \qquad (2.4)$$

As is illustrated in figure 1, this theory does not even approximately agree with the experimental values. The above equation indicates a vacuum for the base pressure at Mach numbers greater than about 2.4. Such a condition is an obvious impossibility. A sufficient reason for the large discrepancy between Gabeaud's theory and experiment is that the base drag at supersonic speeds does not appear in the form of vortex rings in the wake of a body; instead, it appears in the form of shock waves extending laterally from the edge of the wake to distances far into the fluid. Consequently, even though the mechanism pictured by Gabeaud may be approximately correct at low subsonic speeds (since it is the axially-symmetric analogy to the Kármán vortex trail) it must be discarded as a basis for calculation in supersonic flows. In Gabeaud's theory there is, however, an interesting feature which may be in qualitative accordance with experiment even though the theory itself is based on entirely incorrect assumptions. On passing through the speed of sound, the theory indicates a

sudden increase in the base drag. There is some recent experimental evidence for the occurrence of such a phenomenon, but as yet no definite conclusions can be drawn.

About one year after Gabeaud's theory appeared, von Kármán (reference 4) set up a different model for determining the flow over the base. He assumed that the ratio of the velocity of the fluid just outside the dead-air region to the velocity of the projectile was independent of Mach number, and hence equal to the value existing for low-speed flows. If U_b is again the velocity of the fluid just outside the dead-air region, then von Kármán's assumption requires that

$$1 - \frac{U_b^2}{U_\infty^2} = \text{const.} = P_{b_o} = \text{base pressure coefficient at } M_\infty = 0.$$

From the equations for isentropic flow, the pressure coefficient is related to the velocity ratio and the free-stream Mach number by (2.2). Hence the final equation for the base pressure coefficient according to von Kármán's assumption is

$$P_b = \frac{2}{\gamma M_\infty^2}\left[\left\{1 + \frac{\gamma-1}{2} M_\infty^2 P_{b_o}\right\}^{\frac{\gamma}{\gamma-1}} - 1\right] \qquad (2.5)$$

This function is also illustrated in figure 1. The values of P_{b_o} as determined from experiment range from about -0.20 to -0.24. If -0.20 is used (this is the most favorable value to choose for von Kármán's theory), then (2.5) gives the right order of magnitude for the base pressure except at Mach numbers greater than about 4, for which this theory also gives a vacuum. There is no evident reason for the basic assumption on which this theory rests. Von Kármán, himself, terms it as only a "plausible" assumption, without giving any justification for it.

Lorenz, Gabeaud, and von Kármán each had in mind the practical problem of calculating the base drag of a projectile. In retrospect it is somewhat surprising that of the three theories the only one which is even in approximate agreement with experimental measurements on projectiles traveling at Mach numbers greater than about 2.5 is the theory based on the concept of Lorenz—a concept which in principle is known to be completely incorrect. This clearly illustrates that agreement between any phenomenological theory of base pressure and experimental measurements does not necessarily mean that the phenomenological assumptions on which the theory is based are even approximately correct.

The status of the existing theories of base pressure appears, therefore, to be as follows: they give, at best, only the right order of magnitude for the base pressure, and this for only a limited region of supersonic Mach numbers. The many shortcomings of these theories are attributable to the fact that the phenomenological assumptions on which they are based have no sound theoretical foundation.

It is clear that a completely different approach is needed in order to develop a satisfactory theory. Moreover, it is also evident that an exact mathematical treatment of the problem would have to combine the effects of compressibility, viscosity, and pressure gradient—this is certainly out of the question at the present time. Accordingly, two other approaches can be taken:

(1) an exact mathematical treatment can be made of the idealized physical problem of base pressure in an inviscid fluid; or

(2) an approximate mathematical treatment can be made of the actual physical problem of base pressure in a real fluid.

The first approach is the more direct of the two, and is taken up in some detail in part III. Unfortunately, the results of part III indicate that a strictly inviscid-fluid theory cannot possibly be satisfactory. Consequently, the second approach is then taken up in part IV. This latter approach uses dimensional analysis as much as possible, and has for its goal the development of a theory which is based on a minimum number of phenomenological assumptions yet includes all the important variables (Mach number, Reynolds number, type of boundary-layer flow, and body shape) that are expected to have an appreciable effect on base pressure.

PART III. BASE PRESSURE IN AN INVISCID FLUID

Throughout part III the effects of viscosity are completely ignored and the flow field determined for a strictly inviscid fluid. Thus, for the time being, both the existence of boundary-layer flow and the mixing of dead-air with fluid outside a free streamline are excluded from consideration.

1. Two-Dimensional Inviscid Flow

(a) Semi-infinite two-dimensional body. In order to achieve the greatest possible simplicity at the outset, the case of a semi-infinite body will be considered first. By this is meant a body of constant thickness which extends from the base to "minus infinity" (figure 2a). It is assumed throughout this investigation that a dead-air region of constant pressure exists just behind the base. This assumption is necessary, since, if no dead-air existed the flow would have to be deflected 90 degrees by a single shock wave in order to bring the fluid to its original free-stream direction. Such a situation clearly is impossible because no flow can be deflected through more than 46 degrees by a single shock wave.

The present problem, then, is to determine the detailed flow pattern in the neighborhood of the base. Since the effects of viscosity are at present excluded from consideration, the problem is (by symmetry) exactly the same as that of determining the flow over a two-dimensional, flat, horizontal surface which has a step in it (figure 2b).

A reasonable question to ask first is whether or not a possible flow pattern can be constructed which satisfies all

necessary boundary conditions including the requirement that the pressure in the dead-air region be constant. This question is easily answered in the affirmative by constructing such a solution. For example, suppose the free-stream Mach number is 1.50 and some particular value of the base pressure coefficient, say $P_b = -0.30$, is <u>arbitrarily</u> chosen. The base pressure coefficient is defined by

$$P_b = \frac{p_b - p_\infty}{\frac{1}{2}\rho_\infty U_\infty^2} \tag{3.1}$$

where p_b is the base pressure and p_∞, ρ_∞, and U_∞ are, respectively, the pressure, density, and velocity of the free stream. Since the base pressure is prescribed, the initial angle-of-turning through the Prandtl-Meyer expansion at B (figure 2b) is uniquely determined, and in this particular case is equal to 12.4 degrees. The pressure, and hence the velocity and Mach number, must be constant along the free streamline BC. For the particular example under consideration the Mach number along the free streamline is easily calculated to be 1.92. In two-dimensional flow (with no interaction from a second family of Mach waves) the pressure depends only on the angle of inclination of a streamline, hence it follows that BC is a straight line. The triangle BCE is thus a region of uniform flow having the same pressure as the dead-air region. As the trailing shock wave (figure 2b) extends outward from E to infinity, interference from the expansion waves gradually decreases its strength until it eventually becomes a Mach wave. That part of the shock wave from C to E must deflect the flow through the same angle as the expansion waves originally turned it (12.4 degrees for the particular example under consideration). This deflection certainly

is possible since the Mach number in the triangle BCE is 1.92 which, according to the well-known shock relationships, is capable of any deflection smaller than 21.5 degrees. As the flow proceeds downstream from the trailing shock wave CEF, the pressure gradually approaches the free-stream static pressure, thus satisfying the boundary condition at infinity. The shape of the slightly curved shock wave extending from E to infinity is approximately a parabola with focus at the origin of the Prandtl-Meyer expansion wavelets.

It is evident that a possible flow pattern has been constructed which satisfies all the prescribed requirements as well as the necessary boundary conditions. The immediate question to be asked now is whether the particular flow pattern constructed is the only possible one for the particular Mach number (1.50) under consideration. The answer obviously is no, since there is nothing distinguished about the number -0.30 which was arbitrarily chosen for the base pressure coefficient. Any value less (in absolute magnitude) than -0.30 also would have permitted a flow pattern to be constructed and still satisfy all boundary conditions. On the other hand, consider what would happen if values of the arbitrarily-chosen base pressure are gradually decreased from that value corresponding to a base pressure coefficient of -0.30. The angle-of-turning through the Prandtl-Meyer expansion would increase and point C simultaneously would move toward the base. The base pressure can be decreased in this manner only until a condition is reached in which the shock wave at C turns the flow through the greatest angle possible for the particular local Mach number existing along the free streamline. The base pressure cannot be further reduced and still make it

possible for steady flow to exist. The flow pattern corresponding to this limiting condition of a maximum-deflection shock wave can be considered as a "distinguished" flow of all those possible. There are obviously an infinite number of possible flows for a given free-stream Mach number, but only one distinguished flow.

This distinguished or limiting value of the base pressure coefficient can be easily calculated as a function of the free-stream Mach number by inverting the above procedure of constructing possible flow patterns. Thus, for a given value of the local Mach number along the free streamline a distinguished flow pattern can be constructed by simply requiring that the angle-of-turning be equal to the maximum deflection angle possible for a shock wave at that particular local Mach number. The appropriate value of the free-stream Mach number is then directly calculated from the angle-of-turning and the local Mach number along the free streamline. This process can be repeated for different values of the local Mach number along the free streamline and a curve drawn of the limiting base pressure coefficient as a function of Mach number. Such a curve is presented in figure 3. The shaded area represents all the possible values of the base pressure coefficient. For a given Mach number M_∞, the upper bound of the shaded area corresponds to the distinguished flow condition.

There is certainly no reason apriori to say that for a given M_∞ the distinguished flow pattern represents that particular one which most nearly approximates the flow of a real fluid. The curve representing these distinguished flow patterns can be considered simply as being the curve of maximum base drag

possible in an inviscid flow. This is the only interpretation that will be given to this curve for the time being. Since it is these distinguished solutions which will be singled out later for further use, a special symbol P_{b_i} will be used to designate the base pressure coefficient of such flows. It is evident from a comparison of figures 1 and 3 that the values of P_{b_i} for two-dimensional flow correspond to very high base drags, being almost as high as if a vacuum existed at the base. At present there is no experimental data available for two-dimensional bodies, hence any conclusions obtainable from a comparison of inviscid theory and experiment must await future experimental results.

(b) Finite two-dimensional body. A superficial examination of the flow pattern around finite two-dimensional bodies, such as those sketched in figures 4a and 4b, will suffice to show that in two-dimensional flow there is no essential difference between the base pressure for a finite body and that for the semi-infinite body. If the body is made up of several straight-line segments, as in figure 4a, then the base pressure would be exactly that corresponding to a semi-infinite body whose free-stream Mach number is equal to the Mach number M_1 existing in the region of flow that is parallel to the original flow direction (figure 4a). In two-dimensional flow it is also true that to second order in the deflection angles the Mach number M_1 and the pressure p_1 are equal to the corresponding values in the free stream. Hence, for such body shapes the base pressure coefficient is the same (to the second order) as for the semi-infinite body at the same free-stream Mach number.

If the body contour consists of curved lines, as in figure 4b,

the situation is, for all practical purposes, still the same. The Mach number M_1 just ahead of the first expansion wavelet issuing from the base is not quite constant but varies slightly from A to G. It is the Mach number and pressure distribution along the line AG which determines the base pressure coefficient. If the body curvature is not large, then the curvature of the bow shock wave would not be large; hence the influence of the Mach wavelets of the second family of characteristics (those reflected from the bow shock wave) would not be large. The pressure would then depend only on the angle of inclination of the flow, as is the case for the semi-infinite two-dimensional body.

All of the foregoing presupposes that the angle β (figure 4b) is less than the maximum shock-deflection angle possible for the particular Mach number existing along the free streamline BC. If β is larger than this critical value separation would necessarily occur upstream of the base in an inviscid fluid.

In summary, it can be said that, for all practical purposes, the distinguished base pressure coefficient for a finite body in two-dimensional inviscid flow is the same as that for a semi-infinite body. There are, however, an infinite number of possible solutions for each body shape.

2. Axially-Symmetric Flow

(a) Semi-infinite axially-symmetric body. In principle, exactly the same method of procedure can be used for inviscid axially-symmetric flow as was used for inviscid two-dimensional flow. Only the details of the method need to be different;

they will be somewhat more involved and considerably more tedious to carry out than the corresponding two-dimensional-flow calculations. In axially-symmetric flow the expansion wavelets issuing from the corner of the base are not straight lines as they are in Prandtl-Meyer flow. The flow conditions do not depend solely on the inclination of the streamlines at a given point, but depend also on the whole history of the flow upstream of the Mach lines passing through that point. The free streamline cannot be straight but must be curved.

In order to construct possible flow patterns as was done in the two-dimensional case, the method of characteristics must be used and each flow pattern built up step by step. The hodograph net in the velocity plane of each flow pattern must also be built up step by step along with the net of Mach lines in the physical plane. The details of the method of characteristics for axially-symmetric flows will not be explained here as they are described in detail in reference 5.

Using the characteristics method the inviscid flow field corresponding to a given value of the base pressure coefficient can be constructed for any given value of the Mach number. The shape of the free streamline is, of course, determined by the condition that the pressure and hence the velocity must be constant along it. An example of such a construction for a free-stream Mach number of 1.5 is given in figure 5a. In this particular case the base pressure coefficient which has been chosen (arbitrarily) is -0.25. It is to be noted that there is a striking difference between the axially-symmetric case (figure 5a) and the two-dimensional case (figure 2b). The inviscid flow pattern for the axially-symmetric case cannot be

constructed all the way down to the axis of symmetry. This is because the Mach number along the free streamline in the case under consideration is 1.84, which, at the most, is capable of deflecting a streamline only 19.9 degrees by a shock wave. As is illustrated in figure 5a, the angle of inclination of the free streamline for this example is already 19.9 degrees at a value of $r/r_0 = 0.552$, where r is the radial distance from the axis and $r_0 = D/2$ is the radius of the body. Since the angle of inclination of the constant-pressure free streamline would continue to increase monotonically as the axis is approached, the flow pattern of figure 5a cannot be constructed farther than the point shown ($r/r_0 = 0.552$) and still leave a provision for the flow to be deflected through a shock wave and become parallel to the axis of symmetry.

This phenomenon is not a consequence of the particular Mach number and base pressure selected. In figures 5b, 5c, 5d, and 5e several other examples are presented which illustrate the flow for different values of Mach number and for different values of base pressure coefficient. In each case the free streamline has been terminated at the point where the local angle of inclination is equal to the angle corresponding to the greatest possible deflection by a single shock wave. It is evident that none of the flow patterns could be constructed down to the axis of symmetry. Altogether, about five times as many flow patterns were constructed (by the characteristics method) as are shown in figure 5; in no case could the flow be constructed all the way down to the axis.

It is not necessary, however, to discard such flow patterns as useless solutions just because the flow cannot be constructed

all the way to the axis. Instead, the particular flow field of figure 5a, for example, can be considered as a possible flow for a body of revolution which has a rod of diameter $d = 0.552D$ attached to the base and extending along the entire axis downstream to infinity (figure 6). Moreover, if this is done, then the trailing shock wave for such a flow turns the free streamline through the greatest deflection possible for that particular free-stream Mach number. The flow field is therefore the "distinguished" flow field of all those possible for the given Mach number and the given type of configuration shown in figure 6. Just as in the case of the two-dimensional body, there are also an infinite number of possible flow patterns for the body of revolution with a rod attached. This is true because for a given configuration (e.g. figure 5a) as many additional flow patterns as desired can be constructed by simply selecting the base pressure to be any value larger than that corresponding to the distinguished flow.

The distinguished flow pattern is to be given the same physical significance for axially-symmetric flow as it was for two-dimensional flow; i.e., the corresponding base pressure coefficient (P_{b_i}) represents the maximum base drag and hence the maximum entropy increase possible for an inviscid flow about the given configuration.

Clearly, by choosing different values of the base pressure coefficient for a fixed Mach number, the inviscid solutions worked out by the method of characteristics enable a plot of P_{b_i} against d/D to be made. By repeating this procedure for several different values of the free-stream Mach number, P_{b_i} can be determined as a function of both the Mach number and

the ratio d/D. The values of P_{b_i} for d/D = 0 would correspond to the case of the semi-infinite body without any rod attached, and the values for d/D = 1.0 would correspond to the previously treated case of two-dimensional flow.

The procedure outlined above has been carried out for free-stream Mach numbers of 1.25, 1.5, 2.5, and 4.0. The reader will be spared all the tedious details because they are not essential for an understanding of the end results. The final curves of P_{b_i} against d/D for constant values of the Mach number are shown in figure 7. It is to be noted that for each curve the value of P_{b_i} extrapolated to d/D = 0 is so extremely small, even from the most optimistic viewpoint, that it is not even of the same order of magnitude as the experimentally measured values. In fact, on the basis of the curves shown in figure 7, the only possible base pressure coefficient for the inviscid flow over a body of revolution without a rod behind it appears to be zero. This means that the base pressure is equal to the free-stream static pressure and the base drag is zero. The distinguished flow pattern and the infinity of possible flows for d/D > 0 degenerate into a single trivial solution corresponding to zero base drag for d/D = 0.

This result appears anomalous on first thought, particularly when one remembers that the coefficient P_{b_i} represents the maximum possible base drag that can exist in an inviscid fluid. An explanation can be obtained from a consideration of the equations of motion since they are the basis for the method of characteristics. This explanation, however, is not essential for an understanding of the main conclusions regarding base pressure, and hence is presented as Appendix A. It may be noted

here, though, that the considerations given in appendix A also lead to the following generalization of the result just noted for the particular case of base-pressure flows:

> It is impossible for a steady axially-symmetric inviscid supersonic flow to converge toward, and to meet the axis at a finite (non-zero) angle. (3.6)

As explained in appendix A, this statement is to be considered as a conjecture rather than as a rigorously-proven mathematical theorem. Regardless of the extent of mathematical rigor behind the general statement (3.6), it is nevertheless certain that the base-pressure flows for an axially-symmetric body in an inviscid fluid are radically different from those observed in a real fluid. This strongly suggests that viscosity is the essential variable determining the base pressure.

(b) Finite axially-symmetric body. Due to the influence of the ogival nose on any projectile-shaped body, the Mach number M_1 (figure 9a) and the pressure p_1 are different from their respective values M_∞ and p_∞ in the free stream. In contradistinction to the case of two-dimensional flow, this difference would be considerable even if the body were composed of straight-line segments and the afterbody were parallel to the undisturbed flow direction. Actually there is a slight outward gradient in the flow characteristics just ahead of the base (subscript 1), but for practical purposes M_1 and p_1 can be taken as the values averaged from point A to point G (figure 9a). With this interpretation, the base pressure on the finite body (with a rod attached) must be the same as that acting on a semi-infinite body which is immersed in a free stream of Mach number and pressure equal to M_1 and p_1, respectively.

It is clear that when there is no rod behind the body the

same difficulty exists as in the case of the semi-infinite axially-symmetric body; the flow cannot meet the axis of symmetry. This means that the free streamline must eventually become parallel to the axis as it passes downstream, as illustrated in figure 9b. Since the pressure at infinity is equal to the free-stream static pressure, it follows that the only possible base pressure in the strictly inviscid flow is again the free-stream static pressure.

For present purposes it is sufficient to note that, except possibly at very high Mach numbers, the pressure p_1 is less than p_∞. This means that there must be a weak shock at the corner of the base (figure 9b). The free streamline must then curve slightly as it trails downstream to infinity, eventually becoming parallel to the axis.

The solution of figure 9b represents the only type of solution possible for the finite axially-symmetric body. The base drag is zero, but the flow pattern is not what would precisely correspond to a trivial solution (in the mathematical sense of the word), as is the case for the semi-infinite body. Nevertheless, this singular solution for inviscid flow apparently has no bearing on any flow that has as yet been encountered in experimental investigations. Again it appears that viscosity must be the dominating mechanism in determining the flow pattern in a real fluid.

3. Non-Uniqueness of the Inviscid Base-Pressure Flows

The occurrence of more than one possible solution in a flow problem with a fixed body shape is not new. The problem of non-uniqueness arose in the early stages of airfoil theory for an

inviscid, incompressible fluid. As is well known, a satisfactory solution to this particular problem has been found in the use of the so-called Kutta-condition. Thus, of the infinite number of possible solutions for the inviscid flow over an airfoil at a given angle-of-attack, only one corresponds to a finite velocity at the trailing edge. Use of the Kutta-condition to select this particular solution is, therefore, a fairly straightforward process.

When shock waves are allowed in an inviscid compressible flow, it is too often the case that more than one type or location of shock wave is possible within the realm of non-viscous theory. Indeed, in the case of the central problem of this thesis it is possible to fit an infinite number of possible shocks, all different, into a flow field and still satisfy all boundary conditions. Unfortunately, no simple and direct criterion such as the Kutta-condition is known for overcoming these non-uniqueness difficulties which occasionally arise in compressible fluid flows.

Depending on the circumstances, and the particular author, a variety of methods has been used in the past whenever it was necessary to select a suitable flow solution from a possible choice of more than one. The most common factors which have been considered in deciding which flow to select are as follows:

1. Consideration of the stability of the various inviscid flows.
2. Consideration of the second law of thermodynamics or of some not too well defined principle of maximum or minimum entropy.
3. Consideration of the qualitative effects of viscosity or of the qualitative combined effect of viscosity and compressibility.

In the remaining part of this section these three considerations

are separately discussed with particular reference to their possible application to the problem of the infinite number of possible base-pressure flows.

Stability considerations. A relatively simple example of the use of stability considerations is the case of shock waves in a converging-diverging channel. This has been treated by Kantrowitz in reference 6. It is easy to see that for supersonic flow entering a converging-diverging channel there are two possible locations for the shock wave, one upstream of the throat and one downstream. Both solutions to the problem have the same boundary conditions at the extreme ends of the channel. The approximate calculations of Kantrowitz show that when small disturbances (pressure waves) are superimposed on each of these two flows, the resulting motion of the flow with a shock upstream of the throat is unstable, but with a shock downstream the motion is stable. For these two flows, the consideration of stability apparently provides a valid basis for deciding, on purely theoretical grounds, which solution most nearly approximates that occurring in a real fluid.

Recent work in transonic flow has provided another interesting example of how an inviscid flow which satisfies all equations of motion and boundary conditions may, nevertheless, be unstable. In this case, the problem is to determine under what conditions a given type of transonic flow may be expected when two types (one with and one without shock waves) are evidently possible. Guderley (reference 7) maintains, after a rather long and involved mathematical treatment, that the flow without a shock wave is unstable to infinitestimal changes in the boundary contour of the body. From this result Guderley

infers that the smooth-recompression type of flow does not occur in a real fluid.

Although instability in the above cases seems to be an appropriate consideration for maintaining that certain inviscid flows are not physically realizable, it is necessary only to make a few simple observations in order to show that stability in an inviscid fluid is not a valid criterion for choosing one of the infinite number of possible base-pressure flows. Suppose, for example, the flow illustrated in figure 2b were suddenly disturbed in a manner such that point C (intersection of shock and free streamline) would be displaced to a point C'. Then, since a strictly inviscid fluid is not capable of interchange or mixing of the external air and the dead-air, the mass of air in the dead-air space would have to remain constant during the disturbed motion. The dead-air volume would be decreased and its pressure thereby increased over the values existing just outside the free streamline. Thus, the resulting unbalanced forces would cause the point of intersection of shock wave and free streamline to move back toward C. Again, if a disturbance were to cause the steady-state position C to be temporarily shifted to C", then, by the same type of reasoning, it follows that the unbalanced forces would be stabilizing. It is to be concluded, therefore, that the flow is stable even to large disturbances. Since the argument leading to this conclusion holds equally well for any one of the infinite number of possible flows, regardless of Mach number, it is clear that the stability of the inviscid flows does not constitute a valid criterion for selecting any particular one of the possible flows.

Entropy considerations. The use of the second law of

thermodynamics to rule out simple expansion discontinuities in a tube of uniform flow is well known. Mathematically, both compression and expansion discontinuities are possible in an inviscid flow through a straight tube. A discontinuous expansion, however, is accompanied by a decrease in entropy and is therefore ruled out without further consideration. A closer investigation shows that there is, in fact, no mechanism which could bring about an expansion-discontinuity wave.

The second law cannot be used in the base-pressure problem since every possible flow under consideration involves an increase in entropy. The amount by which the entropy is increased varies continuously from zero to a maximum value corresponding to the distinguished flow pattern. Hence, if the magnitude of the entropy increase is used as a criterion for determining which of the infinite number of possible flows most nearly corresponds to the flow of a real fluid, then the condition of maximum entropy increase would necessarily have to be selected in order to avoid choosing the trivial solution of minimum (zero) entropy increase. Such a procedure would single out the distinguished flow patterns. It certainly is not obvious, however, that this procedure is justifiable.

If the system under consideration were a purely mechanical one involving only kinetic and potential energies, then the condition of minimum potential energy would represent the state of dynamic equilibrium, as is well known from experience. Similarly, if the system under consideration were a purely thermodynamic one involving only thermodynamic variables, then it is also known that with the other external variables constant, equilibrium would be attained only when a maximum value of the

entropy is reached. Unfortunately, the flow of a compressible fluid involves an interplay of both dynamics and thermodynamics, and no simple principle for determining steady-state equilibrium is known. Even if such a principle were known, it would likely be based on empirical evidence just as are the above-mentioned laws for dynamics and thermodynamics. Experiments, of course, are necessarily made with viscous, heat-conducting fluids. Therefore, it appears that an entropy principle could be logically used for selecting a solution only after the qualitative effect of viscosity had been considered and shown to still leave more than one possible solution from which to choose. Even without analyzing the qualitative effects of viscosity, it can be seen that the entropy increase alone is not a significant parameter since such a criterion logically would have to be applied to both two-dimensional and axially-symmetric flow. Unfortunately, if d/D is zero, the only possible axially-symmetric inviscid-flow solution from which to choose on this basis is a trivial one.

Viscosity considerations. Even when consideration is given only to the qualitative effects of viscosity, the base-pressure problem is relatively involved. For this reason, these considerations are presented in a subsequent part (part IV) which is concerned with the approximate treatment of base pressure in a real fluid. It may be noted here that, according to the considerations given in part IV, the viscous mixing of dead-air and the outside flow is such as to make possible only one solution for a given Mach and Reynolds number. Accepting this result for the time being, it may be concluded in view of the foregoing consideration on entropy, that the character of maximum entropy

by itself does not justify the selection of a particular inviscid-flow solution from the infinite number of possible ones.

4. Summary of Results of Part III

The foregoing "exact" mathematical treatment of base pressure in an inviscid fluid has furnished two principal results. First, for a given body shape and a given Mach number there are an infinite number of possible solutions both for two-dimensional, and for axially-symmetric flow with a rod attached. Second, for a body of revolution, such as a projectile, without a rod attached to the base, the only possible solution corresponds to zero base drag. Moreover, there is no justifiable basis for selecting one particular flow from the infinite number that are possible at a given Mach number.

These results indicate that viscosity must be the essential variable in determining the base pressure. It is concluded, therefore, that a satisfactory theory of base pressure must necessarily include the effects of viscosity. Since an accurate mathematical treatment of base pressure in a real fluid is at present out of the question, and since the results of an accurate mathematical treatment of the idealized fluid flow are unsatisfactory, the remaining alternative is to develop an approximate theory for a real fluid flow. This is done in part IV.

PART IV. BASE PRESSURE IN A VISCOUS FLUID

Although viscosity has not previously entered the considerations, an important effect of it is already evident from the results of part III. This is the pronounced effect of a rod behind the base of a body of revolution. Thus, the displacement effect of the boundary layer can be expected to have a strong influence in axially-symmetric flow but not in two-dimensional flow. Considerations such as these suggest ways of approximately calculating the base pressure. Before proceeding with the development of a phenomenological theory of base pressure, however, it will prove advantageous first to discuss the qualitative effects of viscosity on the inviscid flow patterns, and then to calculate roughly the displacement effect resulting from the mixing of a supersonic stream and a dead-air space.

1. Qualitative Effects of Viscosity on the Base-Pressure Flow

(a) Two-dimensional flow. A sketch showing the qualitative flow characteristics for the inviscid flow in the region of the base is given in figure 10. The flow starts with a Mach number M_1, pressure p_1, and boundary-layer thickness δ_1. Because the base pressure is considerably lower than the pressure p_1, a small fan of expansion wavelets originates at point A. The existence of a dead-air region in a small volume immediately behind the base is a result of the separation at point B. Hence it may be deduced that the pressure along the streamline BC is approximately constant. For the case of laminar flow in the boundary layer, transition begins somewhere near point D and after passing through the region of the trailing shock wave

the flow in the wake becomes completely turbulent. The qualitative form of the boundary-layer profiles at two stations between points B and C must take on the same nature as those existing at the boundary of a supersonic jet issuing into a room. Because of the viscosity of the fluid, the dead-air is induced into a slow circulatory motion in the directions indicated by the small arrows in figure 10. The resulting mixing process causes the boundary layer to thicken as it approaches point C. Due to the adverse pressure gradient in the neighborhood of the trailing shock wave, the boundary-layer thickness must further increase somewhat as it passes from about point C to point E. The dimension t in figure 10 will be referred to simply as the "wake thickness".

With this qualitative picture of the flow processes in mind, a brief description can be given as to how the base pressure arrives at its steady-state equilibrium value. To fix conditions in mind, suppose a jet of air is pumped from the body into the dead-air region and then is suddenly stopped. At the instant the jet is turned off, point C is far downstream of its equilibrium position. Due to the scavenging effect of the outside flow on the mass of dead-air, some of this dead-air would be removed, thus lowering the pressure of the dead-air region and permitting the angle-of-turning at the corner to be increased. The larger angle-of-turning increases the velocity outside the boundary layer, which in turn increases the scavenging action, thereby again lowering the pressure and starting the cycle over again. Thus, point C moves rapidly to a position as close to the base as possible.

There are, however, at least two factors which prevent

point C from going as far toward the base as that point which roughly represents the maximum-entropy solution for inviscid flow. First, as C moves toward the base the pressure ratio of the trailing shock wave increases, making it more difficult for the scavenged air to overcome the pressure rise of the shock wave and flow downstream. Second, it is likely that some mechanism also occurs near the corner which opposes the turning of a boundary layer through a relatively sharp angle. The individual importance of these two factors which oppose the movement of point C toward the base is not known at present. In any event, it seems clear that some position of equilibrium is soon reached. Hence the qualitative effect of viscosity is such as to select (and slightly modify) one solution from the infinite number of possible ones in an inviscid flow. It is this same qualitative effect of viscosity which justifies the use of the Kutta-condition in airfoil theory. Apparently this phenomenon is quite general.

Returning now to the question of non-uniqueness of the inviscid flows, it is clear that use of the over-all entropy increase as a criterion for selecting one of the inviscid flows cannot be justified, since the qualitative effect of viscosity is to make only one flow possible. Any justification for using the maximum-entropy solution in formulating a theory of base pressure (as is done later on) must come from considerations other than that of the entropy increase alone.

(b) Axially-symmetric flow. Since figure 10 represents only the qualitative flow characteristics near the base, it may be thought of also as representing these characteristics for an axially-symmetric flow. Evidently the same general reasoning

applies here as was used in the two-dimensional case. Compared to the two-dimensional case there is, however, an additional reason for further spreading of the streamlines in the boundary layer as the trailing shock wave is approached. Since the radius of a streamline in the boundary layer continually decreases as the trailing shock wave is approached, further spreading is brought about in order to keep the pressure and cross-sectional area along these streamlines approximately constant.

From figure 7 it is apparent that the displacement effect of the boundary layer is much more important in axially-symmetric flow than in two-dimensional flow. For axially-symmetric flow this effect must be considered in any theory which satisfactorily represents the flow conditions of a real fluid. It is evident, therefore, that the mixing process of the dead-air and the outside stream is of considerable importance. These effects are discussed from a quantitative point of view in a later section which is concerned with the approximate theory of base pressure in a real fluid. (See section 2d.)

2. An Approximate Theory for Base Pressure in a Viscous Fluid

(a) Assumptions of the theory. The qualitative behavior of the base pressure coefficient as a function of boundary-layer thickness can now be determined from the results of the preceding sections. It is clear that for a fixed Mach number the principal variable affecting the base pressure coefficient will be the boundary-layer thickness (δ_1) just ahead of the base. Moreover, when the boundary-layer thickness becomes

large compared to the diameter of the body, the base pressure coefficient must approach zero, i.e., the base pressure must approach the free-stream static pressure. Hence, on a curve showing base pressure as a function of boundary-layer thickness, the portion representing very thick boundary layers can be sketched immediately, as indicated by part CD of the curve in figure 14. However, it is not this part of the curve that is of primary practical interest; rather, it is the portion indicated by BC. Since the wake thickness must approach zero as the Reynolds number is increased indefinitely, it follows that the remaining portion of the curve (from B to A) must come down to the origin for an infinite value of the Reynolds number*. The wake thickness varies quite slowly with Reynolds number, hence the portion AB represents only a small range of δ_1/D, and should be quite steep, as indicated schematically in figure 14.

Figure 14 is only qualitative and therefore may be considered as representing the case of either laminar or turbulent flow in the boundary layer ahead of the base. To be sure, the actual curves may be considerably different in the two cases, but there is no apparent reason for their qualitative shape to be different. For two-dimensional flow, however, the qualitative behavior of the base pressure coefficient for very small values of boundary-layer thickness must be essentially different from that sketched in figure 14, since it is possible

---

* If the boundary layer was removed the portion AB would be considerably different. As long as the Reynolds number is finite, the mixing process would cause the wake thickness to be appreciable even though $\delta_1=0$. In such a case the curve of base pressure coefficient for small values of δ_1/D would be as indicated schematically by the dotted line A'B in figure 14.

for very low base pressures to exist in two-dimensional flow, even in an inviscid fluid.

If it is assumed that the flow separates from the corner of the base and not from a position farther upstream, then for a given type of boundary-layer flow the principal variables of the problem are p_b, p_1, U_1, T_1, δ_1, D, and β, as illustrated in figure 15. It is assumed that only the conditions in the immediate neighborhood ahead of the base affect the base pressure. From dimensional analysis it follows that the above seven variables must be connected by a functional relation involving four independent dimensionless parameters. Hence,*

$$P_b' \equiv \frac{p_b - p_1}{\frac{1}{2}\rho_1 U_1^2} = f\left(M_1, \frac{\delta_1}{D}, \beta\right) \qquad (4.1)$$

Although such a relation may be of some help in correlating experimental measurements, the appearance of the angle of boat-tailing (β) makes further analysis very difficult. Accordingly, only rectangular base shapes ($\beta = 0$) will be considered in the analysis which follows. This leads to the first, and perhaps most fundamental assumption of the theory:

(i) The base pressure coefficient P_b' depends only on the type of boundary-layer flow, the Mach number M_1, and the dimensionless boundary-layer thickness δ_1/D, which exist just upstream of the base.

It is evident from (4.1) that some assumption must be made as to the variation of base pressure coefficient with δ_1/D if

---

* If desired, the dimensionless variable p_b/p_1 could be used in place of P_b'. The variable P_b' has been chosen for the present investigation since it is directly proportional to the base drag, whereas p_b/p_1 is not.

any explicit formulas are to be obtained. For the particular curve sketched in figure 14, an assumption of a straight line for the interval BC appears to be a good approximation. Of course, it is not known that the actual shape of the curve will be very close to that indicated in the sketch, but it is obvious that, at least for some range of values of δ_1/D, a straight line will be a good approximation. It seems desirable, therefore, to simplify the problem by assuming a linear relationship and then justify it by a comparison with experiments. Designating by P_b^* the intercept of the straight line which best approximates the actual curve, the second basic assumption of the theory can be stated as follows:

(ii) At a given Mach number the change in base pressure coefficient ($\Delta P_b = P_b^* - P_b'$) due to the effects of viscosity is proportional to the dimensionless boundary-layer thickness δ_1/D.

One consequence of assumption (i) is that a common basis for comparison can easily be made for different body shapes, because at supersonic speeds the difference between M_1 and M_∞, and between p_1 and p_∞, is practically independent of the viscosity of the fluid and dependent only on the shape of the body. Assumption (i) also implies that the effect of increasing the length of a body (holding all other parameters constant) is in principle the same as the effect of decreasing the Reynolds number of the flow, since both of these effects increase the boundary-layer thickness. It can be foreseen, therefore, that in the subsequent analysis the length-diameter ratio and the Reynolds number (based on body length) combine into a single parameter which depends only on the type of

boundary-layer flow. (See part c of this section.)

Assumption (ii) has many consequences which will soon be elaborated on. In fact, it is essentially this assumption which enables equations to be obtained in closed form expressing the base pressure as a function of Reynolds number. Although the real justification for making assumption (ii) must come from a comparison of theory and experiment, there are certain theoretical considerations which make this hypothesis of linearity appear at least reasonable for all Mach numbers. Thus, if it is assumed that the effects of viscosity on base pressure are governed to a large extent by phenomena occurring near the corner of the base, then assumption (ii) appears quite reasonable. Without being forced, the fluid particles in the boundary layer cannot make the same sudden turn at the base that the fluid particles external to the boundary layer are attempting to make. It is well known in fluid mechanics that the existence of a force along any surface enclosing fluid particles must always show up in the form of a transport of momentum across that surface. For small values of δ_1/D the transport of momentum in the boundary layer is proportional to the thickness of that layer, and hence the quantity ΔP_b should also be proportional to δ_1/D, since it is essentially a force. Of course, experiments are necessary to determine just how wide a range of Reynolds number can actually be covered and still have the curve remain approximately linear. The extent to which the available experiments justify assumption (ii) is discussed in part V.

The foregoing two assumptions are the foundation on which the approximate theory of base pressure is developed. Equations

for the base pressure coefficient are obtained by first using assumption (i) to determine the effect of body shape, and then using assumption (ii) to evaluate the effect of Reynolds number.

(b) Effects of body shape. As was pointed out in part II, the conditions ahead of the base (M_1 and p_1) differ from the free-stream conditions by an amount which can be calculated from the pressure distribution over the body. By definition,

$$P_b' = \frac{p_b - p_1}{\frac{1}{2}\rho_1 U_1^2} = \frac{q_\infty}{q_1}\left[\frac{(p_b - p_\infty) - (p_1 - p_\infty)}{q_\infty}\right] = \frac{q_\infty}{q_1}\left[P_b - P_1\right] \qquad (4.2)$$

where P_b is the base pressure coefficient $\frac{p_b - p_\infty}{\frac{1}{2}\rho_\infty U_\infty^2}$, $\frac{q_\infty}{q_1} = \frac{\frac{1}{2}\rho_\infty U_\infty^2}{\frac{1}{2}\rho_1 U_1^2}$, and $P_1 = \frac{p_1 - p_\infty}{q_\infty}$. The ratio q_1/q_∞ can be written as

$$\frac{q_1}{q_\infty} = \frac{\rho_1 U_1^2}{\rho_\infty U_\infty^2} = \frac{\rho_1}{\rho_o'}\frac{\rho_o'}{\rho_o}\frac{\rho_o}{\rho_\infty}\left(1 + 2\frac{\Delta U}{U_\infty}\right) \qquad (4.3)$$

provided powers of $\frac{\Delta U}{U_\infty} \equiv \frac{U_1 - U_\infty}{U_\infty}$ higher than the first are neglected. In this equation, ρ_o and ρ_o' represent the stagnation densities corresponding to conditions in the free-stream and to conditions just ahead of the base, respectively. Hence if $\Delta M \equiv M_1 - M_\infty$, then it follows that

$$\frac{\rho_1}{\rho_o'}\frac{\rho_o'}{\rho_o}\frac{\rho_o}{\rho_\infty} = \left(\frac{1 + \frac{\gamma-1}{2}M_1^2}{1 + \frac{\gamma-1}{2}M_\infty^2}\right)^{\frac{1}{\gamma-1}}\left(1 - \frac{\Delta p_o}{p_o}\right) = 1 - \frac{M_\infty \Delta M}{1 + \frac{\gamma-1}{2}M_\infty^2} - \frac{\Delta p_o}{p_o} \qquad (4.4)$$

where Δp_o is the loss in total pressure on passing through the bow shock wave, and may ordinarily be neglected except possibly at very high supersonic Mach numbers. From the energy equation

$$\frac{\Delta U}{U_\infty} = \frac{U_1^2 - U_\infty^2}{2U_\infty^2} = \frac{a_\infty^2 - a_1^2}{(\gamma-1)U_\infty^2} = \frac{a_\infty^2}{U_\infty^2}\frac{1}{\gamma-1}\left(1 - \frac{T_1}{T_o}\frac{T_o}{T_\infty}\right)$$

or,

$$\frac{\Delta U}{U_\infty} = \frac{1}{(\gamma-1)M_\infty^2}\left[1 - \frac{1+\frac{\gamma-1}{2}M_\infty^2}{1+\frac{\gamma-1}{2}M_1^2}\right] = \frac{\Delta M}{M_\infty\left(1+\frac{\gamma-1}{2}M_\infty^2\right)} \qquad (4.5)$$

hence the combination of (4.3), (4.4), and (4.5) gives

$$\frac{q_1}{q_\infty} = 1 + \left(\frac{2}{M_\infty} - M_\infty\right)\frac{\Delta M}{1+\frac{\gamma-1}{2}M_\infty^2} - \frac{\Delta p_0}{p_0} \qquad (4.6)$$

The pressure coefficient P_1 is related to ΔM and Δp_0 by

$$P_1 = \frac{p_1 - p_\infty}{\frac{\gamma}{2}p_\infty M_\infty^2} = \frac{2}{\gamma M_\infty^2}\left(\frac{p_1}{p_0'}\frac{p_0'}{p_0}\frac{p_0}{p_\infty} - 1\right) = \frac{2}{\gamma M_\infty^2}\left[\left(\frac{1+\frac{\gamma-1}{2}M_\infty^2}{1+\frac{\gamma-1}{2}M_1^2}\right)^{\frac{\gamma}{\gamma-1}}\left(1-\frac{\Delta p_0}{p_0}\right) - 1\right]$$

$$= -\frac{2\,\Delta M}{M_\infty\left(1+\frac{\gamma-1}{2}M_\infty^2\right)} - \frac{2}{\gamma M_\infty^2}\frac{\Delta p_0}{p_0} \qquad (4.7)$$

Substituting (4.7) into (4.6) yields the relation

$$\frac{q_1}{q_\infty} \equiv 1+\varepsilon = 1 + \left(\frac{M_\infty^2}{2}-1\right)P_1 - \frac{2}{\gamma M_\infty^2}\left(1+\frac{\gamma-1}{2}M_\infty^2\right)\frac{\Delta p_0}{p_0} \qquad (4.8)$$

The equation for base pressure (4.2) is then

$$P_b = P_b'(1+\varepsilon) + P_1 \qquad (4.9)$$

or, since both ε and P_1 are small compared to unity,

$$P_b = (P_b' + P_1)(1+\varepsilon) \qquad (4.10)$$

The quantity ε is ordinarily quite small, hence (4.10) states that the base pressure coefficient is essentially the sum of P_b' and P_1, the former being independent of body shape and the latter being dependent only on body shape. In extreme cases there may be a considerable pressure gradient along the straight cylindrical part of the afterbody. It is for this reason that the coefficient P_1 has been defined as the average

pressure coefficient along the line AG, as indicated in figures 4b, 9a, 10, and 15. Usually the pressure distribution along the surface of the cylindrical afterbody is given, hence the value of P_1 may be taken as the average value which would exist along the length of the dead-air region if the cylindrical part of the body were to replace that dead-air region. Roughly speaking, this procedure corresponds to selecting the value of P_1 which would exist at a distance of about one diameter behind the base. For large length-diameter ratios this averaging technique is not necessary since the gradients are very small on such bodies, but for a body whose base is near the end of an ogival or conical nose, a large error would be introduced if this technique were not followed.

Summarizing the results obtained thus far in this section, assumption (i) allows the base pressure to be separated into two components, one which is affected by viscosity (P_b') and one which is not (P_1). The component P_1, which depends on the body shape and the Mach number, can be calculated from known methods of determining pressure distributions in an inviscid supersonic flow. The next step is to develop an equation for P_b' as a function of the independent variables of the problem.

(c) Effect of Reynolds number. The coefficient P_b' may be written as follows

$$\frac{P_b'}{P_b^*} = 1 - \frac{P_b^* - P_b'}{P_b^*} = 1 - \frac{\Delta P_b}{P_b^*}$$

where P_b^* represents the intercept of the base-pressure curve on the P_b' axis. As long as the afterbody is not boat-tailed, P_b^* is independent of body shape. Using assumption (ii),

$$\frac{P_b'}{P_b^*} = 1 - C_1 \frac{\delta_1}{D} \tag{4.11}$$

where C_1 is a constant which is independent of the viscosity of the fluid, but possibly dependent on the Mach number. It is to be noted that in the equations developed thus far no mention has been made as to whether the boundary layer is laminar or turbulent. According to the assumptions of the theory, (4.11) should be applicable to both cases, with the provision that the constant C_1 may have a different value for laminar flow in the boundary layer than for turbulent. Likewise, P_b^* may be expected to depend on the type of boundary-layer flow.

In developing expressions for δ_1/D as a function of the independent variables of the problem, namely, Reynolds number and length-diameter ratio, the case of laminar flow in the boundary layer will be considered first. From dimensional analysis and the usual considerations of the terms involved in the boundary-layer equations, it follows that

$$D\left(\frac{\delta_1}{D}\right)\sqrt{\frac{U_\infty}{\nu_\infty L}} = f\left(M_\infty, \text{ body shape}\right)$$

Here L, the length of the body, has been selected as the characteristic length for determining the boundary-layer thickness δ_1. Rewriting this equation,

$$\frac{\delta_1}{D} = \frac{L/D}{\sqrt{\frac{U_\infty L}{\nu_\infty}}} f\left(M_\infty, \text{ body shape}\right) = \frac{C_2}{\sqrt{Re}} \frac{L}{D} \tag{4.12}$$

where C_2 is a function of the Mach number and body shape, but independent of viscosity. The body shape affects the boundary-layer thickness principally through the action of the pressure

gradients set up by the particular contour of the body. If the effects of pressure gradient on the thickness of the boundary layer just ahead of the base are negligible compared to the effects of Reynolds number and length-diameter ratio, then (4.12) is applicable to any body shape or length. Hence, for laminar flow in the boundary layer, (4.11) becomes

$$\frac{P_b'}{P_b^*} = 1 - \frac{a_1}{\sqrt{Re}} \frac{L}{D} \qquad (4.13\text{-L})$$

The new constant a_1, which will probably vary somewhat with Mach number, must at present be determined from experimental data.

If the turbulent boundary-layer profile is approximated by a one-seventh power law, it turns out that the ratio δ_1/D is inversely proportional to the one-fifth power of the Reynolds number. (See reference 17, for example.) This result, which has been corroborated by experiments with low-speed subsonic flows, leads immediately to

$$\frac{P_b'}{P_b^*} = 1 - \frac{a_t}{(Re)^{1/5}} \frac{L}{D} \qquad (4.13\text{-T})$$

for turbulent boundary-layer flow. From the above two equations it is evident that an essential difference between the effects of the two types of boundary-layer flow is that the variation of base pressure with Reynolds number is much slower for a turbulent boundary layer than for a laminar one. (See section V.)

Thus far the effects of body shape and viscosity have been separately analyzed. Equations for the base pressure coefficient on a given body are obtained by combining (4.10) and (4.13). For laminar flow in the boundary layer,

$$\frac{P_b}{P_b^*} = \left(1 - \frac{a_l}{\sqrt{Re}}\frac{L}{D} + \frac{P_l}{P_b^*}\right)(1+\varepsilon) \qquad (4.14\text{-L})$$

and for a turbulent boundary layer,

$$\frac{P_b}{P_b^*} = \left(1 - \frac{a_t}{(Re)^{1/5}}\frac{L}{D} + \frac{P_l}{P_b^*}\right)(1+\varepsilon) \qquad (4.14\text{-T})$$

Thus the general problem of determining the base pressure for a body whose length, ogive shape, supersonic Mach number, and Reynolds number are arbitrary, is reduced to the problem of determining the quantities a_l (or a_t) and P_b^* as a function of the Mach number.

It is to be noted that under the assumptions of the theory, equations (4.14-L) and (4.14-T) should be applicable to two-dimensional flow as well as axially-symmetric flow, provided the appropriate values of a_l (or a_t) and P_b^* are used. At present there are no experimental data available on the base pressure of two-dimensional models, but there are some data available on bodies of revolution. Before making a comparison of the above two equations with the experimental data, however, it will be advantageous to develop an approximate method of calculating P_b^* as a function of Mach number.

(d) Effect of Mach number. In order to utilize the inviscid flow patterns (part III, section 2) in estimating the variation of base pressure with Mach number, it is necessary first to estimate the wake thickness. Here there is an essential difference between the cases of laminar and turbulent flow in the boundary layer.

For laminar flow, the boundary layer is usually thin (as compared to the local radius) along most of the free streamline.

One would expect, therefore, that an approximate calculation of the wake thickness could be made by using two-dimensional laminar-mixing calculations and applying a simple area-ratio correction to account for the additional spreading of the streamlines which is brought about by having axial symmetry in the actual problem.

For turbulent flow, the boundary layer is already quite thick as it approaches the base. Moreover, the rate of mixing is very much greater than for the laminar boundary layer. The thickness of the mixing region is of the same order of magnitude as the radius for almost the entire length of the free streamline. Consequently, the application of two-dimensional mixing calculations to the case of turbulent flow cannot be justified. In order to estimate the wake thickness in this case, other methods must be used, such as measuring the wake thickness from schlieren or shadow-photographs of the flow over a projectile. This is done in part V.

For laminar flow in the boundary layer, however, an approximate calculation of the wake thickness can be made without much difficulty. Figure 16 illustrates the pertinent phenomena involved. If the velocity profiles between B and C are assumed to be similar, then from dimensional analysis and analogy to boundary-layer flow it follows that

$$\delta_2 \sqrt{\frac{U_\infty}{\nu_\infty x}} = \delta_3 \sqrt{\frac{U_\infty}{\nu_\infty (x+l)}} = \text{const.} = K \qquad (4.15)$$

for two-dimensional flow at a given Mach number. Here x is the distance upstream from the corner of the base to a hypothetical point where a pure mixing process would have begun in

order to produce a profile of thickness δ_2 at B. The distance ℓ is measured as indicated in figure 16. Equation (4.15) can also be obtained directly from the results given in appendix B.

Relatively large stresses are set up in the dead-air region the instant the boundary layer leaves the corner of the base. Since the dead-air cannot sustain these large shearing stresses, the transformation from the boundary-layer type profile at A to the mixing profile at B (figure 16) must take place rather rapidly. This means that near the corner the rate of mixing is greater than the rate calculated on the assumption of similar profiles. Hence by taking $\delta_2 = \delta_1$ the calculations should tend to underestimate the final thickness δ_3. Using $\delta_2 = \delta_1$, (4.15) can be written as

$$\frac{\delta_3}{D} = \frac{K}{D}\sqrt{\left(\frac{\delta_1}{K}\right)^2 + \frac{\ell \nu_\infty}{U_\infty}} = \sqrt{\frac{C^2 L^2}{Re\, D^2} + \frac{K^2}{Re}\frac{L}{D}\frac{\ell}{D}}$$

where $\frac{C}{\sqrt{Re}} L$ has been substituted for δ_1. Applying a simple area-ratio correction to account for the three-dimensional effect,

$$\left(\frac{t}{D}\right)^2 = 4\,\frac{\delta_3}{D}$$

where t, the wake thickness, is as indicated in figures 10 and 16. Then

$$\left(\frac{t}{D}\right)^4 = \frac{16\,C^2}{Re}\frac{L}{D}\left[\frac{L}{D} + \frac{K^2}{C^2}\frac{\ell}{D}\right] \qquad (4.16)$$

The value of C may be taken as $5.6(1+0.86M_\infty^2)$ according to the calculations of Lees (reference 16). The only remaining unknown in (4.16) is K, the constant of proportionality for laminar mixing of a supersonic stream and a dead-air space. This constant could easily be estimated for low speed flows by

the usual integral methods of treating boundary-layer flow, such as may be found in references 8 and 9, for example. With only slight modifications, these integral methods could be applied to compressible flows if it is assumed that the Prandtl number is unity. As far as the estimation of the wake thickness (when calculating the base pressure) is concerned, such a procedure would be sufficiently accurate.

On the other hand, the "exact" solution to the problem of laminar mixing of a compressible (or incompressible) stream and a dead-air region apparently has not as yet been worked out. This accurate solution is of interest in itself and has applications to problems other than those concerned with base pressure. An understanding of the methods used in the exact solution of this problem is not necessary for the purposes at hand, hence the detailed calculations are given in appendix B. The results of these calculations, presented in figures 12 and 13, yield

$$K = 15\left(1 + .086 M_\infty^2\right)$$

hence $\left(\frac{K}{C}\right)^2 = 7.6$ for all Mach numbers. The thickness of the mixing-layer profile has been arbitrarily taken at the points where the velocity differs by one per cent from its asymptote. As is shown later on, (4.16) underestimates the wake thickness for low supersonic Mach numbers, and overestimates it for very high supersonic Mach numbers.

Perhaps more important than the actual numerical values given by (4.16) is the general trend it indicates for the variation of t/D with Re. As the Reynolds number is increased both the base pressure and ℓ/D decrease; hence the resulting variation of wake thickness must be somewhat slower than the

fourth power of the Reynolds number. This, of course, neglects any effect which may result from interaction of the trailing shock wave and the boundary layer. In any event, (4.16) indicates that the wake thickness should remain reasonably constant over a relatively wide range of Reynolds number.

Suppose, for the time being, that the wake thickness remained exactly constant as the Reynolds number was increased to a very large value. Then the base pressure would approach P_b^* and the flow pattern would approach that corresponding to the inviscid flow over a body with a rod attached. Consequently, as long as the wake thickness is well defined (reasonably steady wake), it may be expected that the value of P_{b_i} (figure 7) corresponding to a value of d/D equal to the wake thickness (t/D), would be approximately equal to P_b^*. Thus,

$$P_b^* \approx P_{b_i} \text{ corresponding to } \frac{d}{D} = \frac{t}{D}. \qquad (4.17)$$

It is to be noted that the only justification claimed for this relation is that it appears very reasonable on the basis of the discussion of the qualitative effects of viscosity given in section 1 of part IV. Equation (4.17) cannot be expected to yield anything more than a rough approximation if the wake thickness and the trailing shock wave are unsteady.

Figure 24 shows some shadowgraphs* of projectiles in free flight. The boundary layer is laminar in figure 24a (M = 1.68) and the wake thickness seems fairly well defined. On the other hand, for the turbulent boundary layer the wake is definitely

---

* These shadowgraphs were made available to the author through the courtesy of A. C. Charters, Ballistic Research Laboratories, Aberdeen, Md.

unsteady at Mach numbers near 1.3, as is illustrated by figure 24b. Fortunately the turbulent wake becomes much more steady at higher Mach numbers; the steadiness is greatly improved at Mach numbers near 1.8, and quite sharply defined at Mach numbers higher than about 2, as is illustrated by figures 24c and 24d, respectively.

Spark photographs are not as yet available for projectiles with laminar boundary-layer flow below a Mach number of 1.5. However, on the basis of the available spark photographs, it may be surmised that for laminar boundary-layer flow the theoretical calculation from (4.17) of Mach number effect on base pressure should be applicable at least in the range of Mach numbers beyond about 1.5 (presuming that the assumptions leading up to (4.17) are correct). For turbulent boundary-layer flow the theory cannot be expected to apply for Mach numbers less than about 1.5, since the wake becomes very unsteady in this region. The extent to which these expectations are verified by experiments is discussed in part V.

PART V. COMPARISON OF THEORY AND EXPERIMENT

Comparison with wind-tunnel data. Unfortunately, the most complete set of wind-tunnel data is classified at the present time. Consequently, a comparison of the theory with the wind-tunnel data is given separately in the form of a confidential addendum to this thesis.

Comparison with free-flight data. The available free-flight experiments are concerned almost entirely with the effects of Mach number on base pressure. Before the theoretical calculation of the effect of Mach number can be made, however, it is necessary first to determine the wake thickness t/D as a function of Mach number. Equation (4.16) for t/D provides an estimate which should be sufficiently accurate for Mach numbers higher than about 2 because of the insensitivity of P_b^* to t/D in this range. For Mach numbers lower than about 2, though, a more accurate estimate is needed. In order to provide such an estimate some measurements of t/D have been taken from approximately fifty spark shadowgraphs* of various projectiles in flight. Figure 20 shows the results of these measurements together with the values indicated by (4.16) for a laminar boundary layer. As is evident from this figure, equation (4.16) underestimates the wake thickness for laminar flow at low Mach numbers and slightly overestimates it at high Mach numbers. The region of underestimation is to be expected for the reasons already given in part IV, section 2d. The good agreement at Mach numbers between 3 and 4 is probably due largely to the manner in which the thickness of the mixing layer was defined. The definition used would tend to overestimate the wake thickness at very high supersonic Mach numbers.

It is now possible to compare the theoretical and experimental values of P_b^*. For a Mach number of 1.5, the wake thickness for laminar boundary-layer flow is approximately 0.55, as indicated

---

* These spark photographs were made available to the author through the courtesy of A. C. Charters, Ballistic Research Laboratories, Aberdeen, Md.

in figure 20. Using this value of the wake thickness, (4.17) and figure 7 yield a value of -0.25 for P_b^*. This latter value compares very well with the value of P_b^* as determined from the intercept of the line representing the experimental wind-tunnel data.

The base pressure coefficient for different Mach numbers (but for a constant Reynolds number and L/D ratio) would be nearly proportional to P_b^* if the constants a_l and a_t appearing in (4.13-L) and (4.13-T) did not depend on the Mach number. As mentioned in section 2c of part IV, it is to be expected that a_l and a_t will vary somewhat with the Mach number. Nevertheless (4.17) should give the right order of magnitude for the base pressure even if it is assumed that these two constants are independent of the Mach number. Figure 21 illustrates the approximate agreement (based on this assumption) between (4.17) and the experimental data of reference 2. These free-flight data are for turbulent boundary-layer flow with the Reynolds number varying from about 2.8×10^6 to 5.6×10^6 over the range of Mach number covered in the firings. From this figure it may be seen that (4.17) does in fact provide a good approximation to the base pressure coefficient at all Mach numbers higher than about 1.5. When future experiments provide information on the variation of a_l and a_t with Mach number, a more stringent comparison with the theory can be made than that shown in figure 21.

PART VI. RESULTS OF THEORY APPLIED TO OTHER PROBLEMS INVOLVING FLOW SEPARATION

Although the available experiments corroborate the theory of part IV quite well, it may develop that certain modifications to the theory will be indicated by future experiments covering a wide range of both Mach number and Reynolds number. When such experiments have clearly outlined the range of validity of the theory, it can then be applied with confidence to yield quantitative information about many related problems involving separation in supersonic flow. A detailed analysis of such problems on the basis of the present status of the theory appears inadvisable at this time for two reasons: first, the variation of the constant a_l (or a_t) with Mach number has not been verified experimentally, and second, there are no experimental data available for two-dimensional flow. Nevertheless, it seems desirable to indicate briefly some possible extensions of the theory as well as to discuss the types of problems (other than the base pressure of projectiles) to which the theory can profitably be applied.

1. Airfoil Shape for Minimum Profile Drag.

It is usually assumed apriori in analyses of airfoil shapes for minimum drag, either for an inviscid or a viscous flow, that the desired contour will have sharp leading and trailing edges. That this assumption is unjustified can easily be seen from the results of part IV. Suppose, for example, that one could find the contour $y = y(x)$ which had the minimum drag possible of all contours with pointed leading and trailing edges $[y(0) = 0,$

$y(c) = 0$]. This contour can be considered as having zero base area. Now suppose that part of the contour aft of the maximum thickness point is modified to a contour $\bar{y}(x)$ which has a trailing edge of height h, as indicated on the upper airfoil shown in figure 22. Then the drag coefficient C_D of the modified airfoil would be

$$C_D = C_{D_m} + \Delta C_{D_B} + \Delta C_{D_F} \tag{6.1}$$

where C_{D_m} is the minimum profile drag possible for contours with pointed trailing edges, and C_{D_F} represents the "fore drag", defined as the total drag minus the base drag (C_{D_B}). Since the trailing edge is originally sharp, the ratio of boundary-layer thickness δ_1 to the height h is originally infinite. Hence for small h,

$$\Delta C_{D_B} = \left(\frac{\partial C_{D_B}}{\partial h}\right)_{h=0} h = h\frac{\delta_1}{c}\left[\frac{\partial P_b}{\partial\left(\frac{\delta_1}{h}\right)}\right]_{\frac{\delta_1}{h}=\infty} = 0$$

The increment in fore drag, however, is not zero since $\left(\frac{\partial C_{D_F}}{\partial h}\right)_{h=0} \neq 0$. In fact, on the basis of linearized theory,

$$C_{D_m} = A\int_0^c \left(\frac{dy}{dx}\right)^2 dx \quad + \quad \text{skin friction}$$

This equation, of course, assumes that flow separation does not seriously alter the "effective shape" of the airfoil over the rear portion. Under conditions where this assumption is valid it follows that

$$\Delta C_{D_F} = A\int_0^c \left\{\left(\frac{d\bar{y}}{dx}\right)^2 - \left(\frac{dy}{dx}\right)^2\right\} dx \tag{6.2}$$

where A is a positive constant which depends on the Mach number, and $\bar{y}$ is the ordinate of the modified airfoil with the blunt trailing edge. If the new shape is obtained by

simply rotating the rear portion of the contour about the maximum thickness point (point O on the upper airfoil in figure 22) until the base is of height h, then

$$\bar{y} = y + x\frac{h}{c-b} = y + \epsilon x \qquad 0<\epsilon=\frac{h}{c-b}\ll 1 \quad (6.3)$$

and by neglecting terms involving ϵ^2, (6.2) reduces to

$$\Delta C_{D_F} = 2A\epsilon\int_b^c \frac{dy}{dx}\,dx = 2A\epsilon(y_c - y_b) = -A\epsilon t \qquad (6.4)$$

where t is the maximum thickness of the airfoil. It is clear from (6.4) that C_{D_F} is negative since $\left(\frac{\partial C_{D_F}}{\partial h}\right)_{h=0} = -\frac{At}{c-b} < 0$, and hence a slightly blunt trailing edge will produce less drag than a sharp one.

In order to estimate the approximate magnitude of the drag decrease that may be expected by using a blunt trailing edge, a particular example will be considered. Suppose that the Reynolds number is about 10^6 and the boundary layer flow is laminar. In order to simplify the calculations, let both airfoils consist of straight-line segments (as indicated by airfoils 1 and 2 in figure 22). Using the subscripts 1 and 2 to denote the original and modified airfoils, respectively, their drag coefficients are

$$C_{D_1} = C_{D_{F_1}} = 4\frac{\theta_1^2}{B} + \text{skin friction} = (1+k)4\frac{\theta_1^2}{B}$$

$$C_{D_2} = C_{D_{F_2}} + C_{D_B} = \frac{\theta_2^2}{B}(2-\eta)^2 + \text{skin friction} - P_b\frac{h}{c}$$

according to the linearized theory. In these equations θ is the thickness ratio of the airfoil, $B = \sqrt{M_\infty^2 - 1}$, k is the fraction of the profile drag attributable to skin friction, and $\eta = \frac{h}{\theta c}$. The fractional decrease in profile drag brought about

by the modified airfoil is

$$\frac{\Delta C_D}{C_D} = \frac{C_{D_1} - C_{D_2}}{C_{D_1}} = \frac{4\theta_1^2 - \theta_2^2(2-\eta)^2 + BP_b\eta\theta_2}{4(1+K)\theta_1^2} \tag{6.5}$$

For the particular case where $M_\infty = 1.5$, $\theta_1 = \theta_2 = 0.1$, and $\eta = 0.4$, the ratio $\frac{\delta_1}{h} = \frac{6.7}{\sqrt{Re}} \frac{1}{\theta\eta}$ is easily calculated to be 0.16, and the ratio k is approximately 0.1. In axially-symmetric flow $P_b \approx \frac{1}{4}P_b^*$ for $\delta_1/D = 0.16$. Using this same ratio, $P_b \approx \frac{1}{4}P_b^*$, for two-dimensional flow, and using $P_b^* = P_{b_i} = -0.54$ for $M_\infty = 1.5$ (figure 3), then (6.5) becomes

$$\frac{\Delta C_D}{C_D} \approx 0.19$$

which is a substantial reduction in profile drag. It is to be noted that the modified airfoil has a higher section modulus than the original double-wedge airfoil. The drag decrease is considerably larger if the comparison between the two airfoil shapes is based on sections of equal bending strength (equal section moduli). For such a comparison,

$$\theta_2^2 = \theta_1^2 \frac{2-\eta}{2-\eta^3}$$

by elementary strength of materials. Substituting this into (6.5) gives

$$\frac{\Delta C_D}{C_{D_1}} = \frac{4 - \frac{(2-\eta)^3}{2-\eta^3} + \frac{BP_b}{\theta_1}\eta\sqrt{\frac{2-\eta}{2-\eta^3}}}{4(1+K)} \tag{6.6}$$

Using the same values of η, M, and θ_1 as above, the drag reduction in this latter comparison is

$$\frac{\Delta C_D}{C_{D_1}} \approx 0.30$$

Experimental investigations should be conducted in order to see if such large savings in drag are actually possible. From the practical point of view a blunt trailing edge might impair control effectiveness, and hence such contours would

probably be most suited for airfoil sections not incorporating control surfaces. However, this is a matter which must be decided upon from the results of experimental investigations.

2. Wind-Tunnel Support Interference

When a body of revolution is tested in a wind tunnel it almost always is supported from the rear by a cylindrical rod. As a result the measured values of base pressure may be considerably affected by the presence of the support. The support interference is a complicated function of the diameter of the support rod, the unobstructed length of the rod, the Mach number, and the Reynolds number. If, as is often the case, the support is long enough so that the only appreciable interference arises from the "diameter-effect" of the rod, then the results of parts III and IV enable an estimate to be made of the order of magnitude of this interference on base pressure.

For a fixed Mach and Reynolds number, an increase in the support diameter d brings about two different effects: first, the wake thickness is increased thereby causing the absolute value of P_b^* to be increased (cf. figure 7), and second, the appropriate dimensionless boundary-layer thickness $\frac{\delta_1}{D-d}$ is increased thereby causing P_b/P_b^* to be increased. These two effects oppositely influence the base pressure, the first tending to decrease it and the second tending to increase it.

If the Mach number is high, say near 3, then the first effect is negligible for all values of the ratio d/D. (See figure 7.) At high supersonic Mach numbers an increase in support diameter can therefore be expected to result in an

increase in the base pressure (a decrease in the absolute value of the base pressure coefficient). This is illustrated schematically in figure 23. The amount of this increase, however, is difficult to estimate since it depends on the effects of viscosity at high Mach numbers—an almost completely unexplored field.

For intermediate Mach numbers, say near 2, the two above-mentioned opposing effects of an increase in support diameter would largely compensate one another if the values of d/D are not large. In such cases the interference normally would not be an important consideration.

If the supersonic Mach number is low, say near 1.5, then for small values of the ratio d/D the first effect predominates and an increase in support diameter will result in a decrease in base pressure, as illustrated in figure 23. For very large values of the ratio d/D, the second effect must of course predominate and an increase in support diameter will then result in an increase in base pressure. As $d/D \to 1$, the base pressure approaches a value approximately equal to p_1.

Using equation (4.13) and the curves in figure 7, the order of magnitude of the interference in the important region of low supersonic Mach numbers can easily be estimated. Such an estimate indicates that for Mach numbers near 1.5 (or slightly lower) approximately a 20-30 per cent increase in base drag coefficient may occur as a result of the presence of a moderately large support ($d/D \approx 0.6$). Thus it is clear that support interference in this region of low supersonic Mach numbers should be given careful consideration. Unfortunately, support

interference measurements have not been made in most of the existing wind-tunnel investigations. Accordingly, it is not surprising that these experimental results are often inconsistent.

CONCLUSIONS

In the course of the investigation the following general conclusions have been drawn:

(1) The existing theories of base pressure are unsatisfactory either for predicting the base pressure or for correlating experimental measurements.

(2) The exact inviscid-fluid theory of base pressure does not adequately describe the actual phenomenon involved, particularly for axially-symmetric flow. Non-uniqueness difficulties occur in the inviscid base-pressure flows, and apparently there is no simple way in which they can be overcome.

(3) Viscosity is the essential mechanism in determining the base pressure, at least in axially-symmetric flow.

The following specific results have been obtained from an analysis of base pressure in an inviscid fluid:

(4) For a given body shape and a given free-stream Mach number there are an infinite number of possible solutions (each satisfying all necessary boundary conditions) both for two-dimensional, and for axially-symmetric flow with a rod attached to the base.

(5) For inviscid axially-symmetric flow without a rod attached to the base only one solution is possible, but it corresponds to zero base drag.

This latter result is believed to be a special case of a more general result which is conjectured as follows: it is impossible for a steady axially-symmetric inviscid supersonic flow to converge toward, and to meet the axis at a finite (non-zero) angle.

The approximate theory developed for practical applications to base-pressure problems in a viscous fluid indicates that:

(6) At a given Mach number, the base pressure on a body without boat-tailing can be expressed as the sum of two components, one of which is independent of viscosity but dependent on body shape, and the other which is dependent only on viscosity.

(7) The effects of length-diameter ratio and Reynolds number can be combined into a single parameter which depends only on the type of boundary-layer flow.

(8) The variation of base pressure with Reynolds number is slower for a turbulent boundary layer than for a laminar one.

(9) A substantial decrease in profile drag of two-dimensional airfoils is possible by designing the airfoil contour with a blunt trailing edge.

(10) The effect of support interference on base pressure measurements in a supersonic wind-tunnel depends to a great extent on the Mach number, and is most important in the lower region of supersonic velocities.

APPENDIX A. AXIALLY-SYMMETRIC FLOWS CONVERGING TO THE AXIS

In order to explain the rather anomalous result obtained in part III, section 2, it is advantageous to first consider the basic equations of motion on which the method of characteristics is based. The familiar differential equation for the velocity potential of an inviscid axially-symmetric compressible flow is

$$\left(1-\frac{\varphi_x^2}{a^2}\right)\varphi_{xx} - 2\,\frac{\varphi_x\varphi_r}{a^2}\,\varphi_{xr} + \left(1-\frac{\varphi_r^2}{a^2}\right)\varphi_{rr} + \frac{\varphi_r}{r} = 0 \qquad \text{(A.1)}$$

where x is the coordinate measured parallel to the direction of the undisturbed stream and r is the radial coordinate. If a transformation is made to a new system (ξ , η) of curvilinear coordinates, where ξ and η are distances measured along the two Mach lines issuing from a point, then the equation of motion for the velocity potential becomes simply (the details of the algebra involved in making this transformation may be found in reference 5, § 21)

$$\frac{\partial^2\varphi}{\partial\xi\,\partial\eta} = \frac{\sin^2\alpha}{r}\,\frac{\partial\varphi}{\partial r} \qquad \text{(A.2)}$$

where α is the local Mach angle. It is to be noted that the new variables have the simple physical significance that lines of ξ = constant and η = constant are the Mach lines of the flow. The derivative of the velocity potential in any given direction is the projection of the velocity vector along that direction, and the order of differentiation in (A.2) can be interchanged. Hence by letting

$$\frac{\partial\varphi}{\partial\xi} = p \qquad\qquad \frac{\partial\varphi}{\partial\eta} = q \qquad \text{(A.3)}$$

and

$$\frac{\partial \varphi}{\partial r} = v = w \sin\theta$$

where w is the velocity vector inclined at an angle θ with respect to the axis, it follows that

$$dp = \frac{\sin^2\alpha}{r} v\, d\eta \qquad\qquad dq = \frac{\sin^2\alpha}{r} v\, d\xi \qquad\qquad (A.4)$$

Thus, dp is the increment in the projection of the velocity vector along the ξ direction when passing a distance $d\eta$ in the physical plane along the η direction, and dq is the increment in the projection of the velocity vector in the η direction when passing a distance $d\xi$ along the ξ direction. Equations (A.4) are the fundamental equations used in the step-by-step construction of a supersonic flow by Sauer's method of characteristics.

The reasons for the singular behavior as the flow approaches the axis of symmetry can now be explained with the help of (A.4). Suppose a series of steps were laid off in the physical plane in the manner indicated by the sketch shown in figure 8a. The small increments ($d\xi$ and $d\eta$) along the Mach lines are laid off such that they are always small compared to the distance from the axis r and also such that $d\xi/r$ and $d\eta/r$ are always very nearly equal to a constant for all steps. If it were necessary to express the length of these steps more precisely they could be written as

$$\frac{d\xi}{r} = \epsilon\left[1 + \mathcal{O}(\epsilon)\right] = \frac{d\eta}{r} \qquad \text{where} \quad \epsilon \ll 1$$

It is necessary to consider only the order of magnitudes in the following discussion; hence such factors as $\left[1 + \mathcal{O}(\epsilon)\right]$ which

would otherwise appear throughout are omitted for the sake of simplicity. It is to be noted that if such a flow converging to the axis is possible, then there would be an infinite number of such steps along the streamline AB in figure 8a.

Now consider the increments in the hodograph plane corresponding to those laid off in the physical plane (figure 8a). Figure 8b illustrates the way according to (A.3) and (A.4) in which such increments must be laid off in the hodograph plane. Points having the same number in figures 8a and 8b represent the same point in the flow. Let the smallest average Mach angle along the steps in the physical plane be α_m, and the smallest vertical velocity component be v_m, then

$$dp > v_m \epsilon \sin^2 \alpha_m = \text{constant}$$

and

$$dq > v_m \epsilon \sin^2 \alpha_m = \text{constant}$$

for all of the steps along AB. This means that every increment in the hodograph plane is greater than a constant value. This value cannot be zero unless points 1 and 3 are identical, which would represent the exceptional case of a "reversed" conical flow. On passing from point A to point B there are, however, an infinite number of such increments. They must be laid out along the arc of a circle in the hodograph plane since AB is a streamline of constant pressure. This means that before reaching point B the inclination angle of the velocity vector must be greater than 46 (or even 90) degrees. Because this situation obviously prevents a shock wave from being fitted into the flow, a contradiction results with the assumption that such a flow is possible. Hence no such flow can be possible.

It is realized that the foregoing argument would not be termed a rigorous mathematical proof. Such a proof of the above result seems at this time to be quite difficult, particularly when one considers that the governing equations are necessarily non-linear. The preceding discussion does, however, point out the reason for the inclination angle Θ of the streamline increasing at an excessive rate as the axis is approached. The source of the trouble is inherently tied up with the last term in the equation of motion (A.1), since it has r in the denominator and a non-vanishing factor in the numerator. The equations of irrotationality, momentum, and continuity which combine to form (A.1) can written separately as

$$\frac{\partial w}{\partial n} - w\frac{\partial \theta}{\partial s} = 0 \qquad \underline{\text{irrotationality}}$$

$$\frac{\partial w}{\partial s} + \frac{a^2}{\rho w}\frac{\partial \rho}{\partial s} = 0 \qquad \underline{\text{momentum}} \text{ (plus irrotationality)}$$

$$\frac{1}{\tan^2\alpha}\frac{\partial w}{\partial s} - w\frac{\partial \theta}{\partial n} - \frac{w\sin\theta}{r} = 0 \qquad \underline{\text{continuity}} \text{ (plus momentum and irrotationality)}$$

where S is a distance measured along the streamline, and n is a distance measured normal to the streamline. It is evident from these equations that the appearance of r in the denominator of both (A.4) and (A.1) stems entirely from the continuity equation. This leads to a qualitative explanation of the observed behavior near the axis of the inviscid base-pressure flows. Consider the changes that must occur on going from, say, point 1 to point 3 in the physical plane (figure 8a). If the flow were two-dimensional, then the free streamline would be straight and Θ_1 would equal Θ_3, thereby preserving the cross-

sectional area between two adjacent streamlines on passing from 1 to 3. The term involving 1/r does not occur for plane flow and no difficulties arise. In the axially-symmetric case, the fundamental condition is again that the cross-sectional area between adjacent streamlines must be preserved, since $w_1 = w_3$. This means that adjacent streamlines spread apart as the axis is approached. In order to have the pressure at point 3 equal equal to that at point 1, the free streamline curves toward the axis, permitting adjacent streamlines to spread, thereby allowing the continuity equation to be satisfied. Because of the 1/r term in the continuity equation, the curvature increases more and more as the axis is approached. Hence, even before the axis is reached, the inclination of the free streamline exceeds the largest value which any oblique shock wave can possibly overcome.

The foregoing considerations easily lend themselves to several other interesting extensions. If, for example, the particular flow under consideration were not irrotational, then an additional term would appear on the right side of each of equations (A.4). These additional terms would involve the rotation but not the radius r, and hence would have a normal behavior as the axis is approached. Rotation would have no effect on the arguments which followed (A.4). The impossibility of base-pressure flows converging to the axis must, therefore, be extended to include flows with or without rotation.

If the particular flow under consideration in figure 8a were the flow over a solid body instead of a base-pressure flow, then once again only slight modifications in the preceding argument would become necessary. Thus, in figure 8b, instead of AB tracing out an arc of a circle in the hodograph, it would

trace out a line very nearly parallel to the velocity vector, since Θ is approximately constant along AB. Point 3 in the physical plane of figure 8a would then be determined by the point labeled 3' in the hodograph plane of figure 8b. Again, there would be an infinite number of finite steps in the hodograph plane, and they would not, in general, necessarily form a convergent sequence. This means that before reaching the axis the Mach number would be decreased too much to allow a shock wave to deflect the flow back to the original direction of the free stream. An exception, as remarked before, is the case of "reversed" conical flow wherein point 3' coincides with point 1 in the hodograph plane. Even in this exceptional case where the flow can be constructed down to the axis there is no apparent way in which the flow field can be constructed any farther, since a shock wave cannot be fitted into the conical flow pattern in order to make the over-all flow possible. These considerations lead to the following conjecture which has already been stated in part III:

> It is impossible for a steady axially-symmetric inviscid supersonic flow to converge toward, and to meet the axis at a finite (non-zero) angle. (3.6)

This has the interesting consequence that the inviscid supersonic flow over a thin body of revolution pointed at both ends (without cusps) is, in general, not possible without separation occurring somewhere along the surface of the body.

APPENDIX B. LAMINAR MIXING OF A SUPERSONIC STREAM AND A DEAD-AIR REGION

In order to make the laminar-mixing problem amenable to calculation, the usual assumptions will be made that the layer affected by viscosity is thin and has zero pressure gradient along the direction parallel to the main stream (figure 11). The Navier-Stokes equations of motion for the steady flow of a viscous compressible fluid are (in cartesian tensor notation)

$$\rho u_\kappa \frac{\partial u_i}{\partial x_\kappa} = -\frac{\partial p}{\partial x_i} + \frac{\partial}{\partial x_\kappa}\left[\mu\left(\frac{\partial u_i}{\partial x_\kappa} + \frac{\partial u_\kappa}{\partial x_i}\right)\right] - \frac{2}{3}\frac{\partial}{\partial x_i}\left(\mu \frac{\partial u_\kappa}{\partial x_\kappa}\right)$$

In view of the assumptions made above, the Navier-Stokes equation for $i = 1$ ($x_1 = x$, $u_1 = u$) simplifies to the familiar boundary-layer equation

$$\rho u \frac{\partial u}{\partial x} + \rho v \frac{\partial u}{\partial y} = \frac{\partial}{\partial y}\left(\mu \frac{\partial u}{\partial y}\right) \qquad \underline{\text{momentum}} \qquad (B.1)$$

while the equations for $i = 2$ and $i = 3$ ($x_2 = y$, $x_3 = z$, $u_2 = v$, and $u_3 = w$) reduce to zero on both sides. The equation giving the balance of energy for the steady flow (without the addition of external heat) of a viscous compressible fluid with coefficient of viscosity μ, coefficient of heat conduction λ, and specific heat at constant pressure c_p, is

$$\rho u_\kappa \frac{\partial (c_p T)}{\partial x_\kappa} = u_\kappa \frac{\partial p}{\partial x_\kappa} + \frac{\partial}{\partial x_\kappa}\left(\lambda \frac{\partial T}{\partial x_\kappa}\right) + \mu\left[\frac{\partial u_i}{\partial x_\kappa}\left(\frac{\partial u_i}{\partial x_\kappa} + \frac{\partial u_\kappa}{\partial x_i}\right) - \frac{2}{3}\left(\frac{\partial u_\kappa}{\partial x_\kappa}\right)^2\right]$$

In view of the assumptions made, this equation reduces to the usual energy equation for laminar boundary-layer flow

$$\rho u \frac{\partial (c_p T)}{\partial x} + \rho v \frac{\partial (c_p T)}{\partial y} = \frac{\partial}{\partial y}\left(\lambda \frac{\partial T}{\partial y}\right) + \mu\left(\frac{\partial u}{\partial y}\right)^2 \qquad \underline{\text{energy}} \qquad (B.2)$$

In addition to equations (B.1) and (B.2) the equation expressing conservation of mass is needed.

$$\frac{\partial(\rho u)}{\partial x} + \frac{\partial(\rho v)}{\partial y} = 0 \qquad \underline{\text{continuity}} \quad \text{(B.3)}$$

For a given gas the variation of μ and C_p with temperature is known, hence the foregoing system of equations is completed by the addition of the equation of state

$$\frac{T}{T_\infty} = \frac{\rho_\infty}{\rho} \qquad \text{(B.4)}$$

In order to solve the above system of equations, the following assumptions will be made:

(i) All velocity profiles in the mixing region are similar.

(ii) C_p = constant.

(iii) The Prandtl number, $Pr = \frac{C_p \mu}{\lambda} = 1$.

(iv) $\frac{\mu}{\mu_\infty} = \left(\frac{T}{T_\infty}\right)^n$ where n is approximately 0.76 for air.

The first two of these assumptions are almost always made. The third assumption introduces an appreciable error into the temperature profile if the actual Prandtl number of the fluid is much different from unity, as is the case for air where Pr = 0.733. For the purposes at hand, however, only the velocity profile is desired. At moderate supersonic Mach numbers the use of Pr = 1 does not introduce more than about two per cent error in the velocity profile. The small difference between the velocity distributions of laminar boundary layers for Pr = 1 and Pr = 0.733 is clearly shown by the calculations of Emmons and Brainerd (reference 10). Accordingly, in the present calculations assumption (iii) will not appreciably affect the final velocity distributions.

As was first pointed out by Prandtl in reference 11, and later used to advantage by Busemann and Crocco (references 12

and 13, respectively), the consequence of assumption (iii) when applied to boundary-layer flow is that the temperature becomes a function only of the velocity. Thus

$$C_p T = f(u) \tag{B.5}$$

Substituting (B.5) into (B.2) and using (B.1) in conjuction with assumption (iii), it follows that the energy equation is automatically satisfied if

$$f'' + 1 = 0$$

Integrating this equation, using the boundary conditions

$$T = T_\infty \quad \text{for} \quad u = U_\infty$$

$$T = T_d \quad \text{for} \quad u = 0$$

gives

$$f(u) = C_p T = C_p T_d - \frac{u^2}{2} + \frac{u}{U_\infty}\left[C_p(T_\infty - T_d) + \frac{U_\infty^2}{2}\right] \tag{B.6}$$

as the relationship between velocity and temperature. The temperature of the dead-air region T_d will be approximately equal to the stagnation temperature of the free stream. Since the temperature determines the density, (B.6) enables the density to be calculated as a function of the velocity.

Following the method first given by von Mises (reference 14) and later used by von Kármán and Tsien (reference 15), a transformation is made to a new set of independent variables (ψ, x) where ψ is the stream function. By using ψ as one of the independent variables the continuity equation (B.3) is identically satisfied, and the velocity components are given by

$$u = \frac{\rho_\infty}{\rho}\frac{\partial \psi}{\partial y} \qquad v = -\frac{\rho_\infty}{\rho}\frac{\partial \psi}{\partial x} \tag{B.7}$$

The only equation now remaining to be satisfied is the momentum

equation (B.1). The formulas for making the transformation to the new coordinate system are*

$$\left(\frac{\partial}{\partial y}\right)_x = \frac{\partial \psi}{\partial y}\left(\frac{\partial}{\partial \psi}\right) + \frac{\partial x}{\partial y}\left(\frac{\partial}{\partial x}\right) = \frac{\rho u}{\rho_\infty}\left(\frac{\partial}{\partial \psi}\right)_x$$

$$\left(\frac{\partial}{\partial x}\right)_y = \frac{\partial \psi}{\partial x}\left(\frac{\partial}{\partial \psi}\right) + \frac{\partial x}{\partial x}\left(\frac{\partial}{\partial x}\right) = -\frac{\rho v}{\rho_\infty}\left(\frac{\partial}{\partial \psi}\right)_x + \left(\frac{\partial}{\partial x}\right)_\psi \qquad \text{(B.8)}$$

It follows that

$$\rho u\left(\frac{\partial u}{\partial x}\right)_y + \rho v\left(\frac{\partial u}{\partial y}\right)_x = \rho u\left(\frac{\partial u}{\partial x}\right)_\psi$$

and

$$\mu\left(\frac{\partial u}{\partial y}\right)_x = \mu \frac{\rho u}{\rho_\infty}\left(\frac{\partial u}{\partial \psi}\right)_x$$

Hence the momentum equation in the (x , ψ) system becomes

$$\rho_\infty \frac{\partial u}{\partial x} = \frac{\partial}{\partial \psi}\left(u \mu \frac{\rho}{\rho_\infty} \frac{\partial u}{\partial \psi}\right) \qquad \text{(B.9)}$$

This can be put in dimensionless form by introducing the variables

$$u^* = \frac{u}{U_\infty} \qquad \mu^* = \frac{\mu}{\mu_\infty}$$

$$x^* = \frac{x}{L} \qquad \psi^* = \frac{\psi}{\sqrt{U_\infty L \nu_\infty}} \qquad \text{(B.10)}$$

$$\rho^* = \frac{\rho}{\rho_\infty}$$

where ν_∞ is the kinematic coefficient of viscosity and L is any characteristic length. For the sake of simplicity L could be taken as unity if desired. In dimensionless form (B.9) becomes

$$\frac{\partial u^*}{\partial x^*} = \frac{\partial}{\partial \psi^*}\left(\rho^* u^* \mu^* \frac{\partial u^*}{\partial \psi^*}\right) \qquad \text{(B.11)}$$

---

* Occasionally the variables held constant in a differentiation process will be indicated in order to avoid ambiguity.

According to the similarity hypothesis (i) it is necessary that $u^* = u^*(\zeta)$ where ζ is some dimensionless variable involving both ψ^* and x^*. Hence $\zeta = \psi^{*p} x^{*q}$ where p and q are pure numbers which must be determined by the condition that both sides of (B.11) are functions of ζ only. Letting

$$g(\zeta) = \rho^* u^* \mu^* \tag{B.12}$$

then the right side of (B.11) can be written as

$$\frac{\partial}{\partial \psi^*}\left(g(\zeta)\frac{du^*}{d\zeta}\frac{\partial \zeta}{\partial \psi^*}\right) = \frac{\partial}{\partial \psi^*}\left(g(\zeta)\frac{du^*}{d\zeta} p \psi^{*p-1} x^{*q}\right) = x^{*q}\frac{\partial}{\partial \psi^*}\left(g(\zeta)\frac{du^*}{d\zeta} p \psi^{*p-1}\right)$$

from which it is obvious that in order for the right side of (B.11) to be a function only of ζ, it is necessary that $p = 1$. With $p = 1$ (B.11) reduces to

$$q x^{*-2q-1} \zeta \frac{du^*}{d\zeta} = \frac{d}{d\zeta}\left(g(\zeta)\frac{du^*}{d\zeta}\right)$$

Therefore, in order for the entire equation to be a function only of ζ, it is also necessary that $q = -\frac{1}{2}$, hence

$$\zeta = \frac{\psi^*}{\sqrt{x^*}} = \frac{\psi}{\sqrt{U_\infty \nu_\infty x}} \tag{B.13}$$

The ordinary differential equation for the velocity distribution now reduces to

$$-\frac{\zeta}{2}\frac{du^*}{d\zeta} = \frac{d}{d\zeta}\left(g(\zeta)\frac{du^*}{d\zeta}\right) \tag{B.14}$$

In the form written, this is a linear differential equation whose solution can be obtained by two simple quadratures:

$$u^* = C_1 \int_0^\zeta \frac{F}{g}\, d\zeta + C_2 \tag{B.15}$$

where

$$F = e^{-\int_0^{\zeta} \frac{\zeta}{2g}\, d\zeta} \tag{B.16}$$

The boundary conditions are

$$u^* = 1 \quad \text{at} \quad \zeta = \infty$$

$$u^* = 0 \quad \text{at} \quad \zeta = -\infty$$

hence

$$u^* = C\int_0^{\zeta} \frac{F}{g}\, d\zeta + u_o^* \tag{B.17}$$

where u_o^* is the value of u^* at $\zeta = 0$. The constant C must satisfy

$$C = \frac{1 - u_o^*}{\int_0^{\infty} \frac{F}{g}\, d\zeta} = \frac{u_o^*}{\int_{-\infty}^{0} \frac{F}{g}\, d\zeta} \tag{B.18}$$

Equation (B.17) is an integral equation for u^*, since both F and g are functions of u^*. By simply estimating a reasonable solution for u^* as a function of ζ, a first approximation ${}_1u^*$ to the true solution is then

$${}_1u^* = C\int_0^{\zeta} \frac{{}_oF}{{}_og}\, d\zeta + {}_ou_o^*$$

The zero order approximations ${}_oF$ and ${}_og$ can be calculated directly from ${}_ou^*$ by using

$$g(\zeta) = \rho^* u^* \mu^* = T^{*^{n-1}} u^*$$

in conjunction with (B.6). If this process is repeated until the k$^{\underline{th}}$ approximation is the same as the (k-1)$^{\underline{st}}$ approximation (to the degree of accuracy desired), and (B.18) is simultaneously satisfied, then the solution to the problem is obtained.

The iteration process turns out to be rapidly convergent

and three or four iterations are sufficient to obtain the function $u^* = u^*(\zeta)$. In order to change this back to the physical coordinates (x,y) a simple quadrature is necessary. By definition of the stream function,

$$\left(\frac{\partial \psi}{\partial \zeta}\right)_x d\zeta + \left(\frac{\partial \psi}{\partial x}\right)_\zeta dx = d\psi = \left(\frac{\partial \psi}{\partial y}\right)_x dy + \left(\frac{\partial \psi}{\partial x}\right)_y dx$$

or, by using (B.7) and (B.13),

$$\sqrt{U_\infty \nu_\infty x}\, d\zeta + \frac{1}{2}\zeta \sqrt{\frac{U_\infty \nu_\infty}{x}}\, dx = \frac{\rho u}{\rho_\infty} dy - \frac{\rho v}{\rho_\infty} dx$$

Hence, with x held constant, integration gives

$$y\sqrt{\frac{U_\infty}{\nu_\infty x}} = \int_0^\zeta \frac{T^*}{u^*} d\zeta$$

from which $\frac{u}{U_\infty}$ as a function of $y\sqrt{\frac{U_\infty}{\nu_\infty x}}$ can be determined. It is to be noted that no graphical or numerical differentiations are needed in the above iteration process — only quadratures are required.

Numerical calculations have been carried out for two cases:

(1) $M_\infty = 0$ (incompressible flow)

(2) $M_\infty = 2.0$, $T_d = T_o = T_\infty\left(1 + \frac{\gamma-1}{2} M_\infty^2\right)$, $\mu = \mu_\infty \left(\frac{T}{T_\infty}\right)^{0.76}$

The results are shown in figure 12. The effect of increasing the Mach number is simply to increase the thickness of the mixing region. This increase in thickness is due to the heating effect of compressibility which causes the density to be decreased and hence the distance between streamlines to be increased. Since this is the same mechanism which increases the thickness of the boundary layer along a flat plate, one would expect that the ratio $\delta_M / \delta_{M=0}$, where δ is the "thickness" of

the boundary layer, would be approximately equal in the two types of laminar flow. That this actually is the case, at least for $M_\infty \approx 2.0$, is illustrated in figure 13. The curve in this figure represents the known increase of boundary-layer thickness for flow over a flat plate. This curve is represented by

$$\frac{\delta_M}{\delta_{M=0}} = 1 + .0857 M_\infty^2$$

according to Lees (reference 16). As is evident from figure 13, the point representing the thickness for the laminar mixing process falls very near the curve representing the thickness for boundary-layer flow along a flat plate.

REFERENCES

1. Lorenz, H., "Der Geschosswiderstand," Physikalische Zeitschrift, Vol. 18, p. 209 (1917); Vol. 29, p. 437 (1928)

2. Charters, A. C., and Turetsky, R. A., "Determination of Base Pressure from Free-Flight Data," Ballistic Research Laboratories, Rep. No. 653 (March 1948).

3. Gabeaud, "Sur la résistance de l'air aux vitesses ballistiques," Comptes Rendus de l'Academie des Sciences, Vol. 192, p. 1630 (1931).

4. Kármán, Th. von, and Moore, N. B., "The Resistance of Slender Bodies Moving at Supersonic Velocities," Transactions of the American Society of Mechanical Engineers, Vol. 54, p. 303 (1932).

5. Sauer, R., Theoretische Einführung in die Gasdynamik, Julius Springer, Berlin, 1943. Reprinted by J. W. Edwards Bros., Inc., Ann Arbor, Michigan.

6. Kantrowitz, A., "The Formation and Stability of Normal Shock Waves in Channel Flows," NACA TN No. 1225 (March 1947).

7. Guderley, G., "On the Transition from a Transonic Potential Flow to a Flow with Shocks," Wright Field Report AMC, T-2 No. F-TR-2160 ND (1946).

8. Loitsianskii, L. G., "Integral Methods in the Theory of the Boundary Layer," NACA TM No. 1070 (1944).

9. Liepmann, H. W., and Laufer, J., "Investigations of Free Turbulent Mixing," NACA TN No. 1257 (August, 1947).

10. Emmons, H. W., and Brainerd, J. G., "Effect of Variable Viscosity on Boundary Layers, with a Discussion of Drag Measurements," Transactions of the American Society of Mechanical Engineers (Quarterly Journal of Applied Mechanics), Vol. 64, pp. A1-A6 (March, 1942).

11. Prandtl, L., "Eine Beziehung Zwischen Wärmeaustausch und Strömungswiderstand der Flussigkeiten," Physikalische Zeitschrift, Vol. 11, p. 1072 (1910).

12. Busemann, A., "Gasdynamik," Chapter 1, par. 9, in Handbuch der Experimentalphysik, Vol. 4, part I, Akademische Verlagsgesellschaft, Leipzig, 1931.

13. Crocco, L., "Transmission of Heat from a Flat Plate to a Fluid Flowing at a High Velocity," NACA TM No. 690 (1932).

14. Mises, R. von, "Bemerkung zur Hydrodynamik," ZAMM, Vol. 7 (1927).

15. Kármán, von Th., and Tsien, H. S., "Boundary Layer in Compressible Fluids," Journal of the Aeronautical Sciences, Vol. 5, No. 6 (April 1938).

16. Lees, L., "The Stability of the Laminar Boundary Layer in a Compressible Fluid," NACA TN No. 1360 (1947).

17. Prandtl, L., and Tietjens, O. G., Applied Hydro- and Aeromechanics, McGraw-Hill, New York, 1934, p. 76.

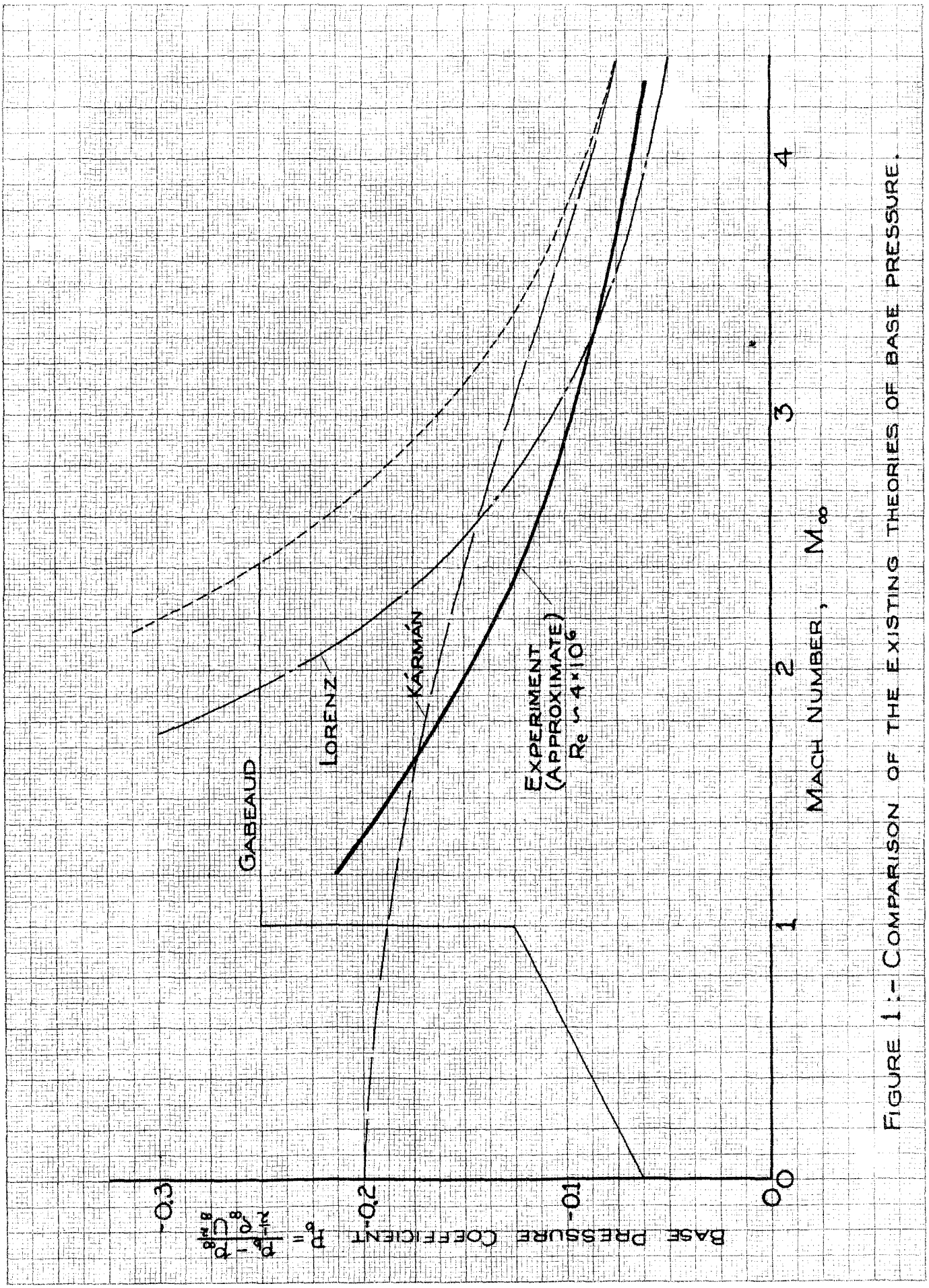

Figure 1:- Comparison of the existing theories of base pressure.

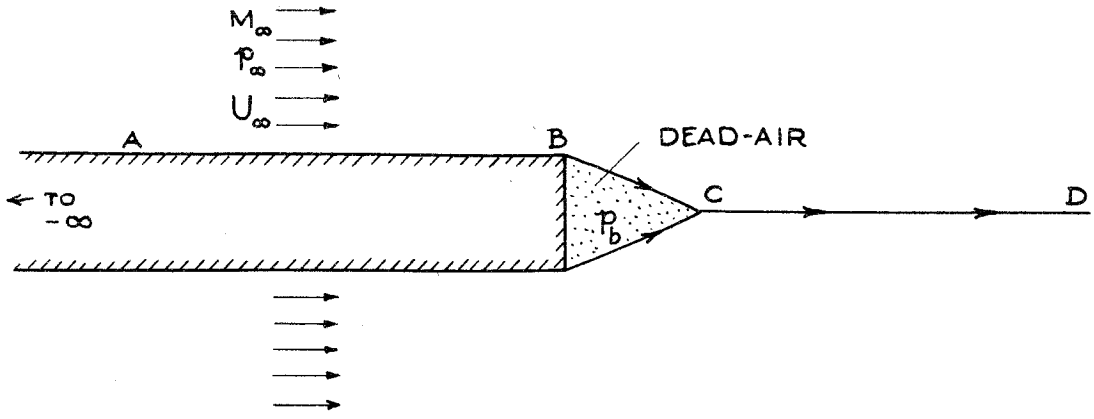

FIGURE 2a:- SEMI-INFINITE BODY

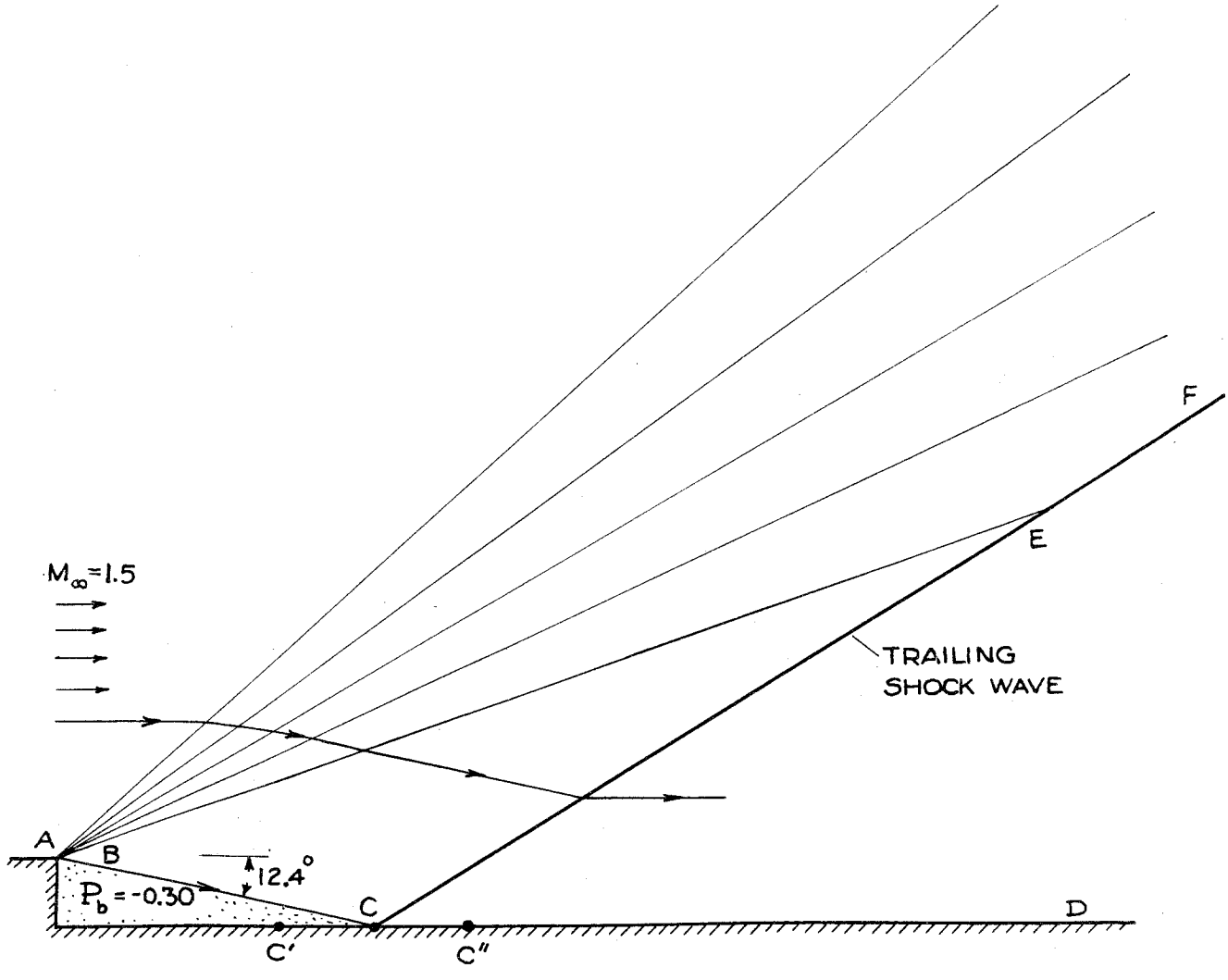

FIGURE 2b:-TWO-DIMENSIONAL FLOW OVER SEMI-INFINITE BODY

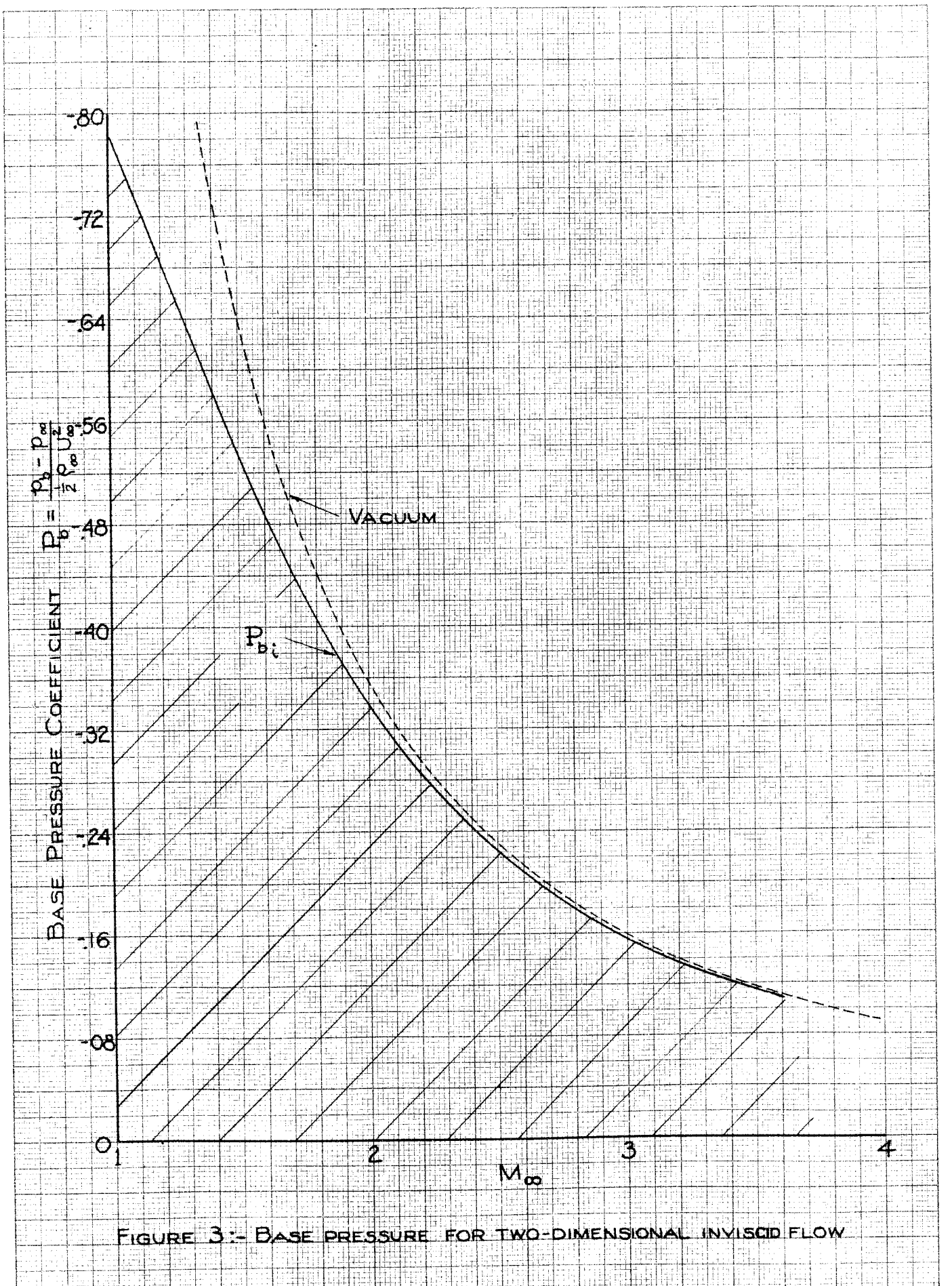

FIGURE 3:- BASE PRESSURE FOR TWO-DIMENSIONAL INVISCID FLOW

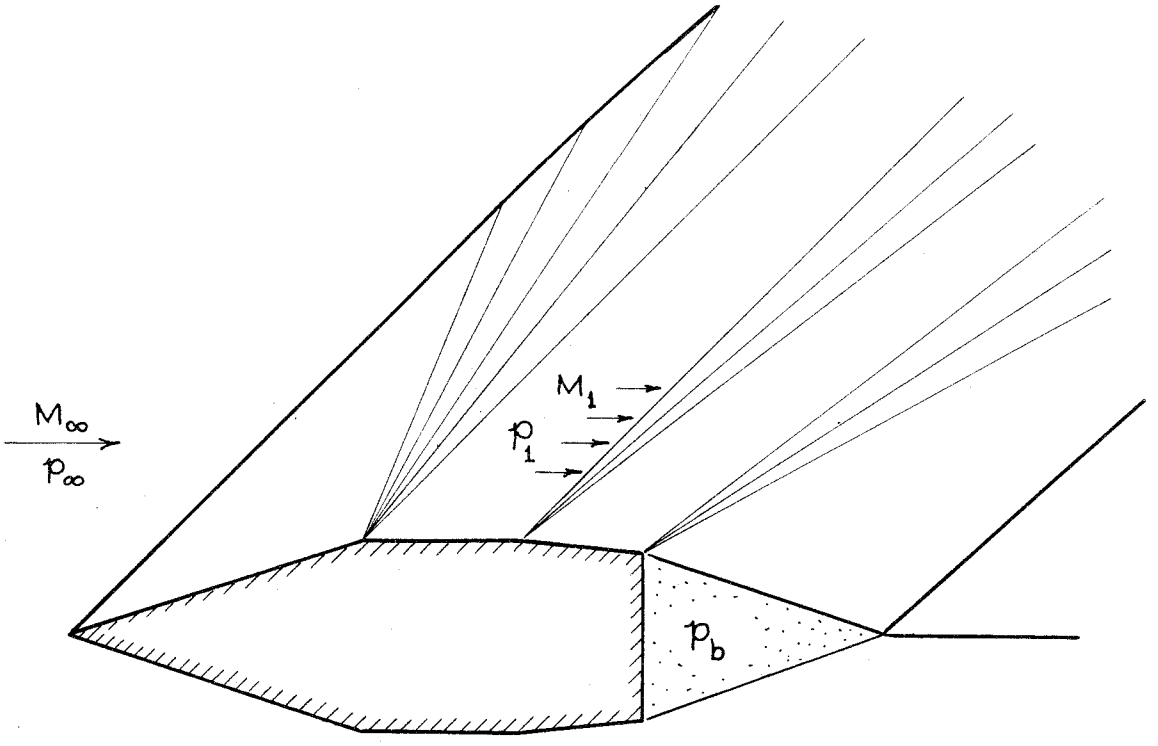

FIGURE 4a:- TWO-DIMENSIONAL BODY WITH STRAIGHT SIDES

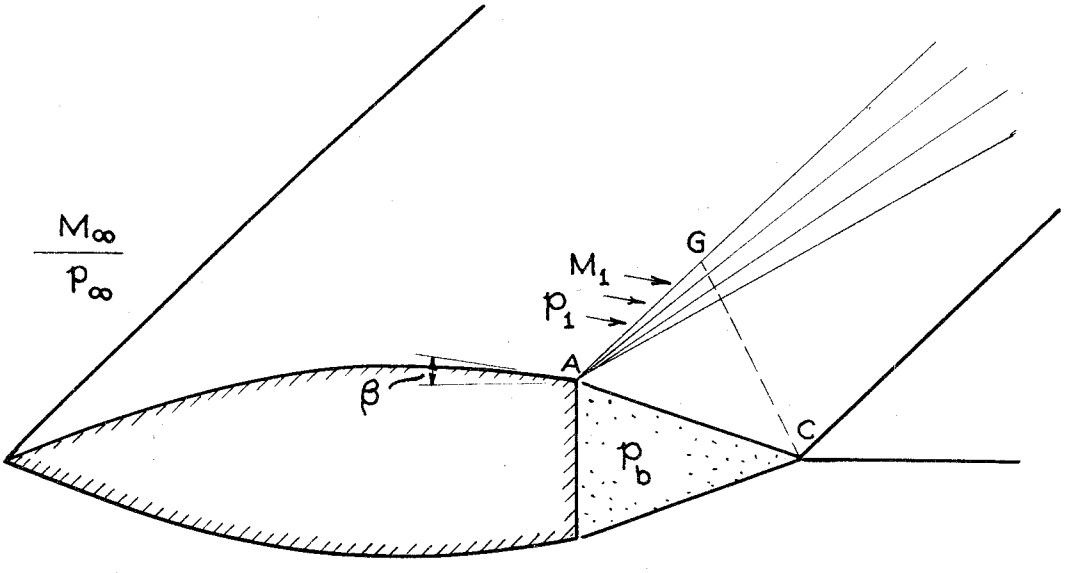

FIGURE 4b:- TWO-DIMENSIONAL BODY WITH CURVED SIDES

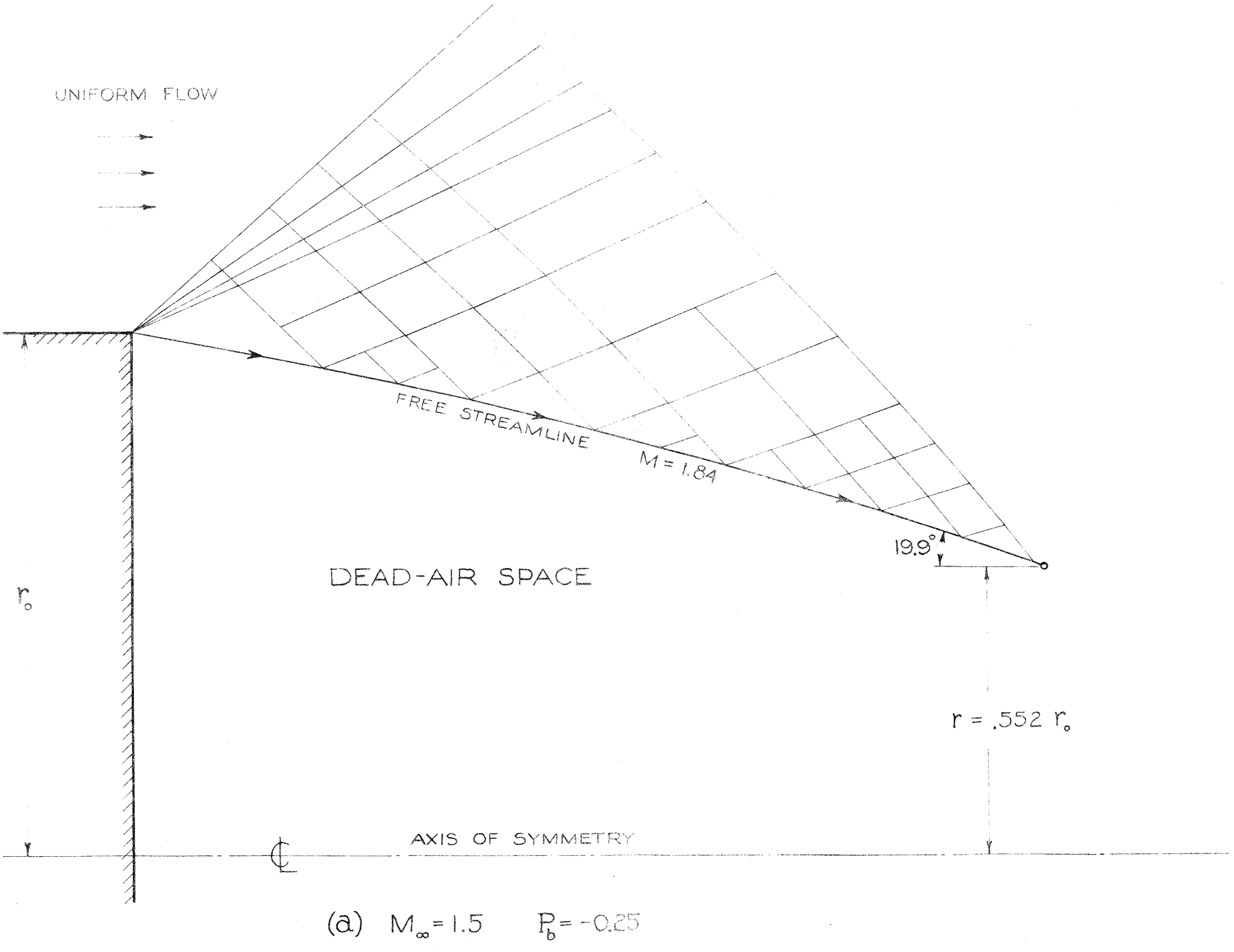

FIGURE 5:- TYPICAL MACH NETS FOR INVISCID FLOW OVER THE BASE

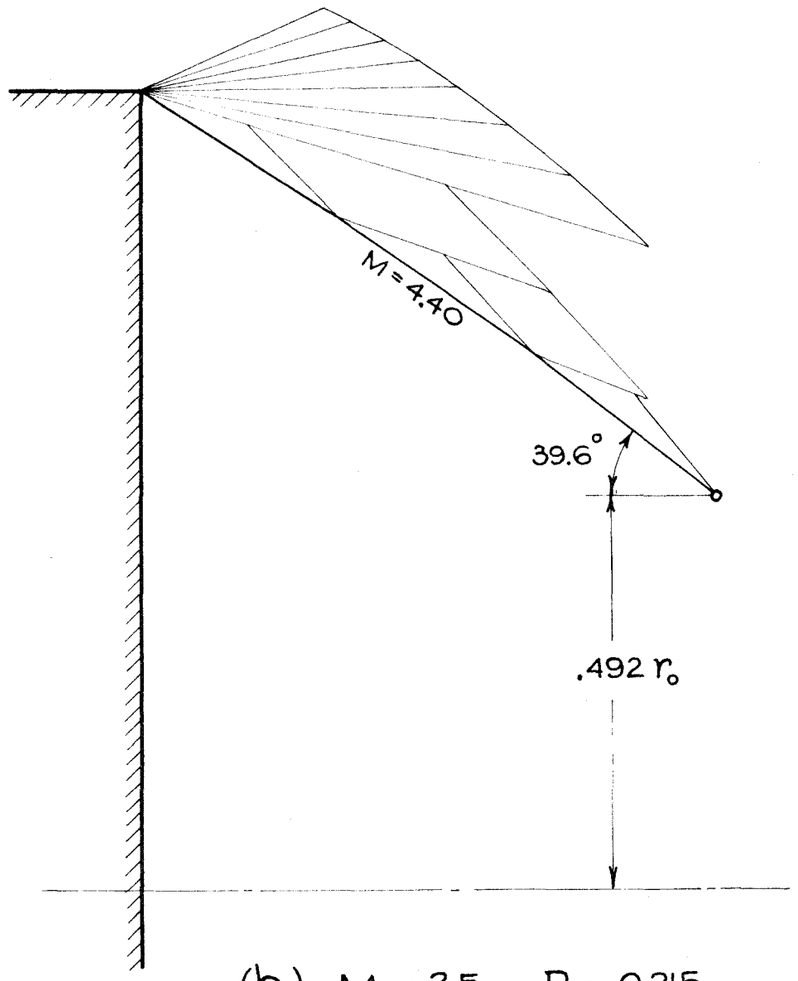

(b) $M_\infty = 2.5$ $P_b = -0.215$

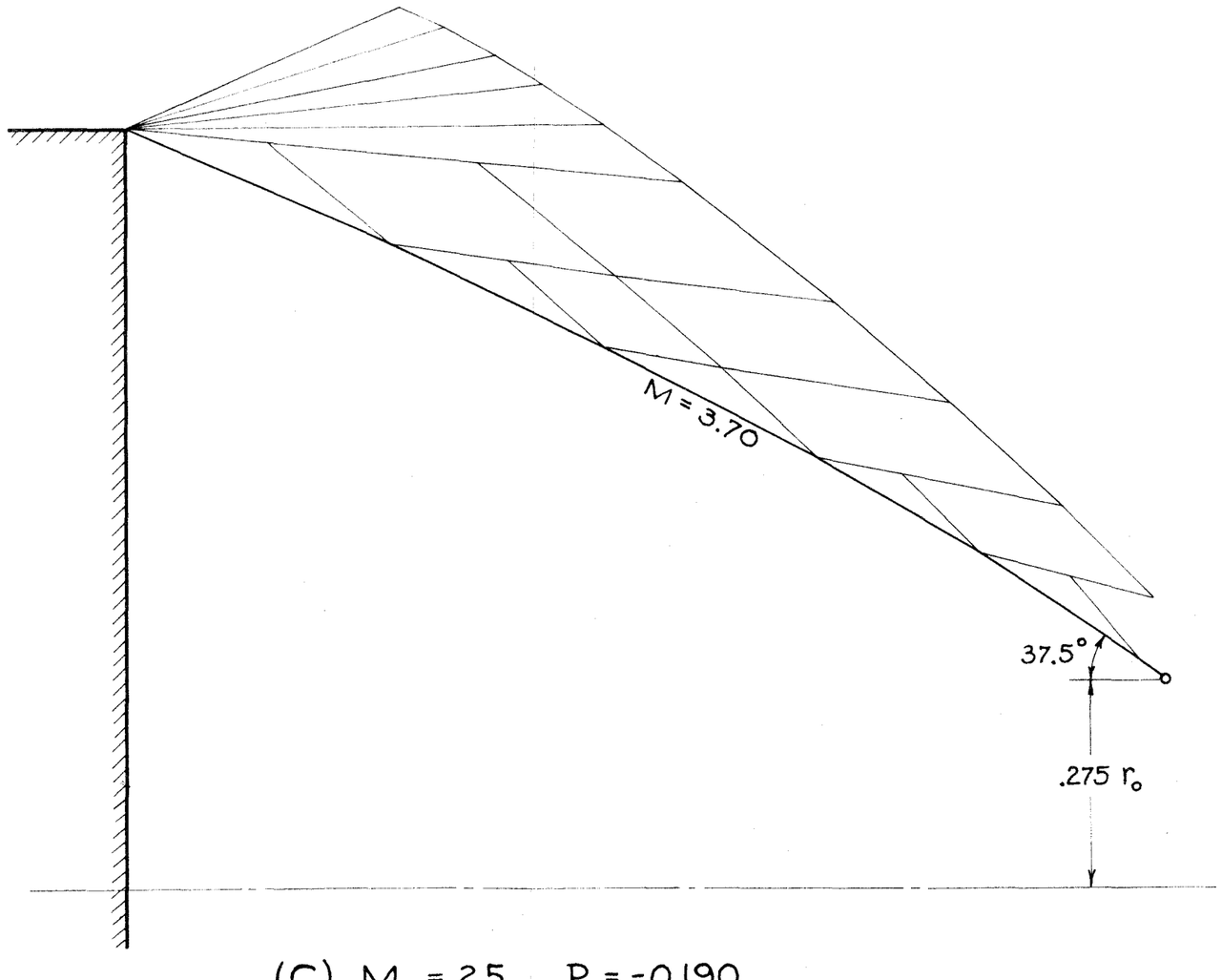

(C) $M_\infty = 2.5$ $P_b = -0.190$

FIGURE 5:- CONTINUED

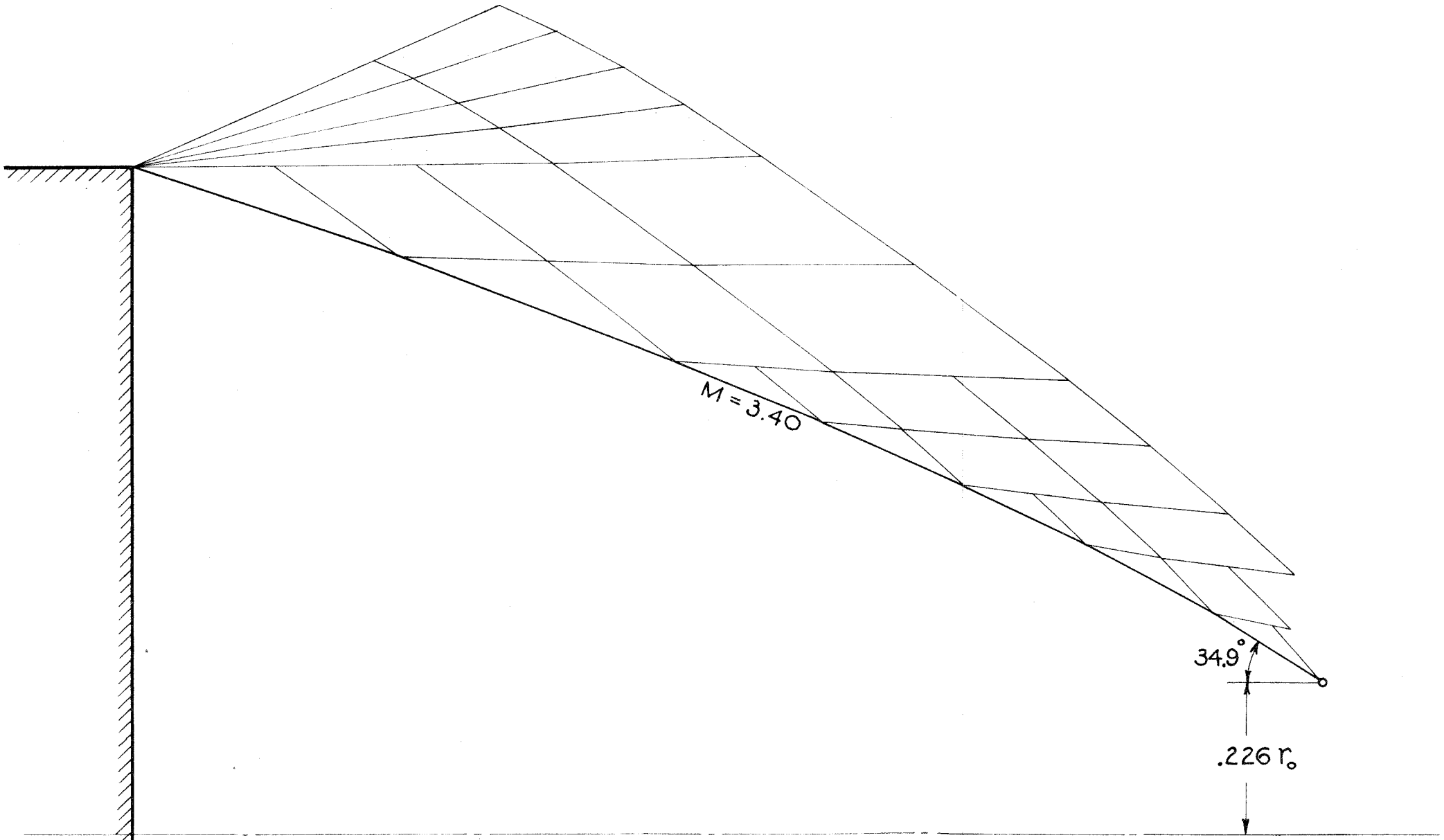

(d) $M_\infty = 2.5$ $P_b = -0.170$

FIGURE 5:- CONTINUED

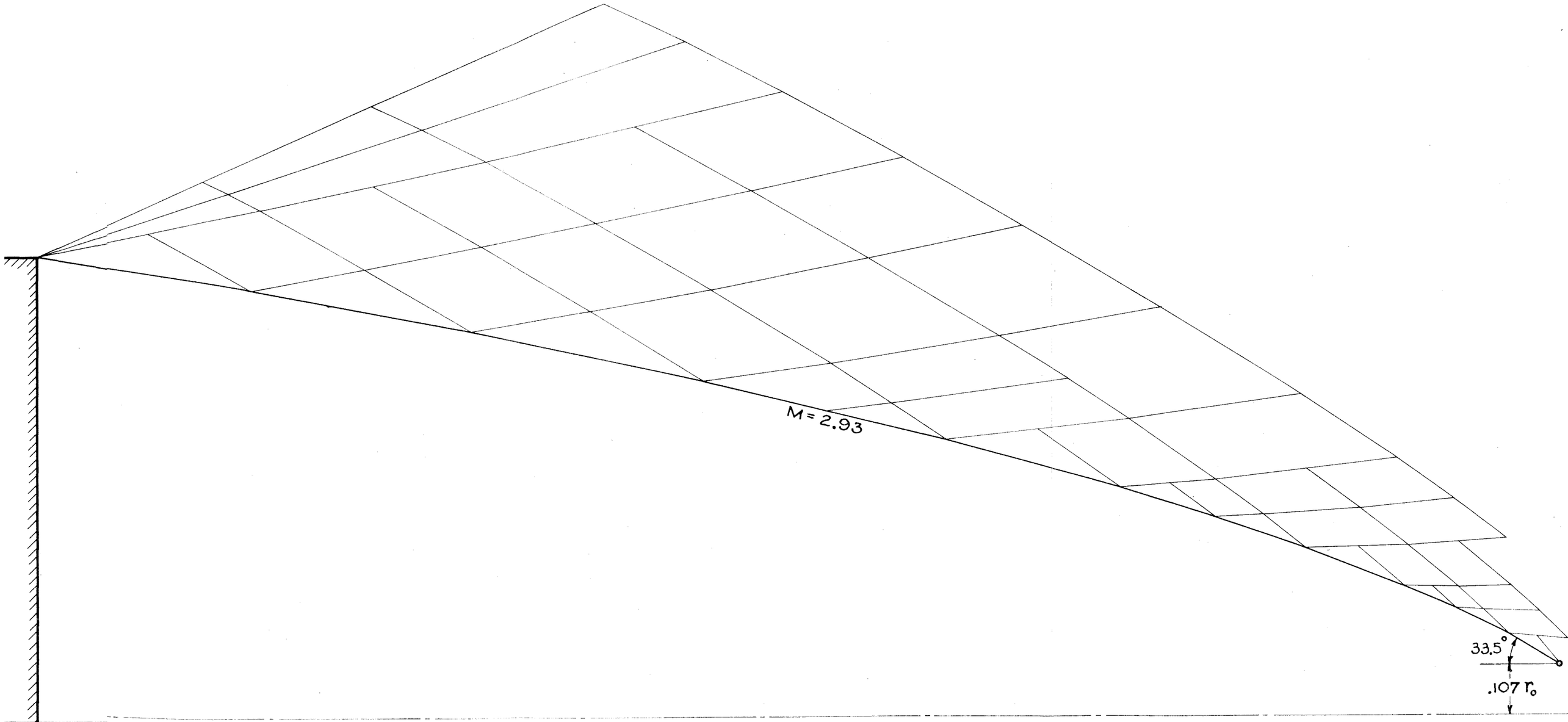

(e) $M_\infty = 2.5$. $P_b = -0.11$

FIGURE 5 :- CONTINUED

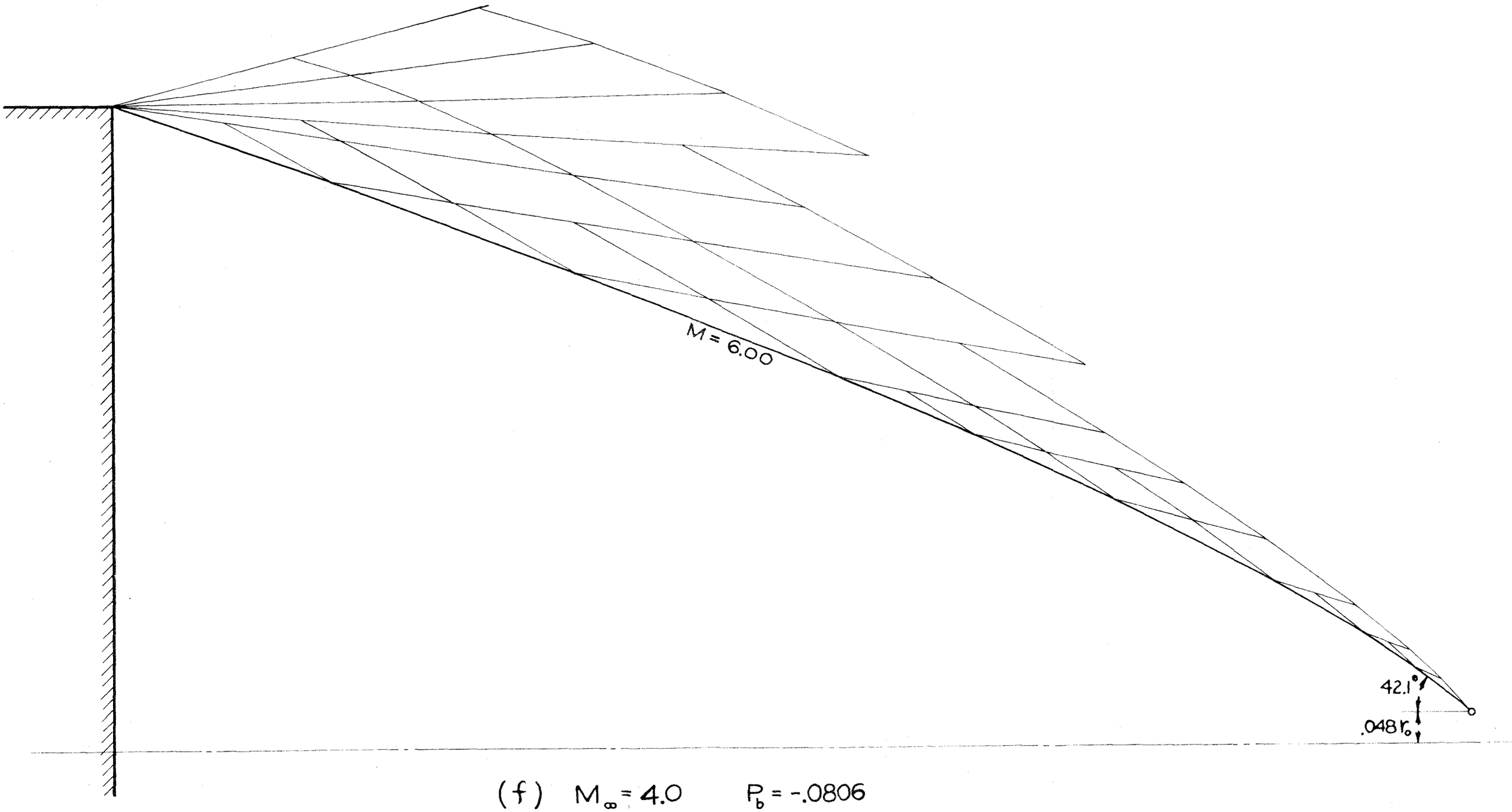

(f) $M_\infty = 4.0$ $P_b = -.0806$

FIGURE 5:- CONCLUDED

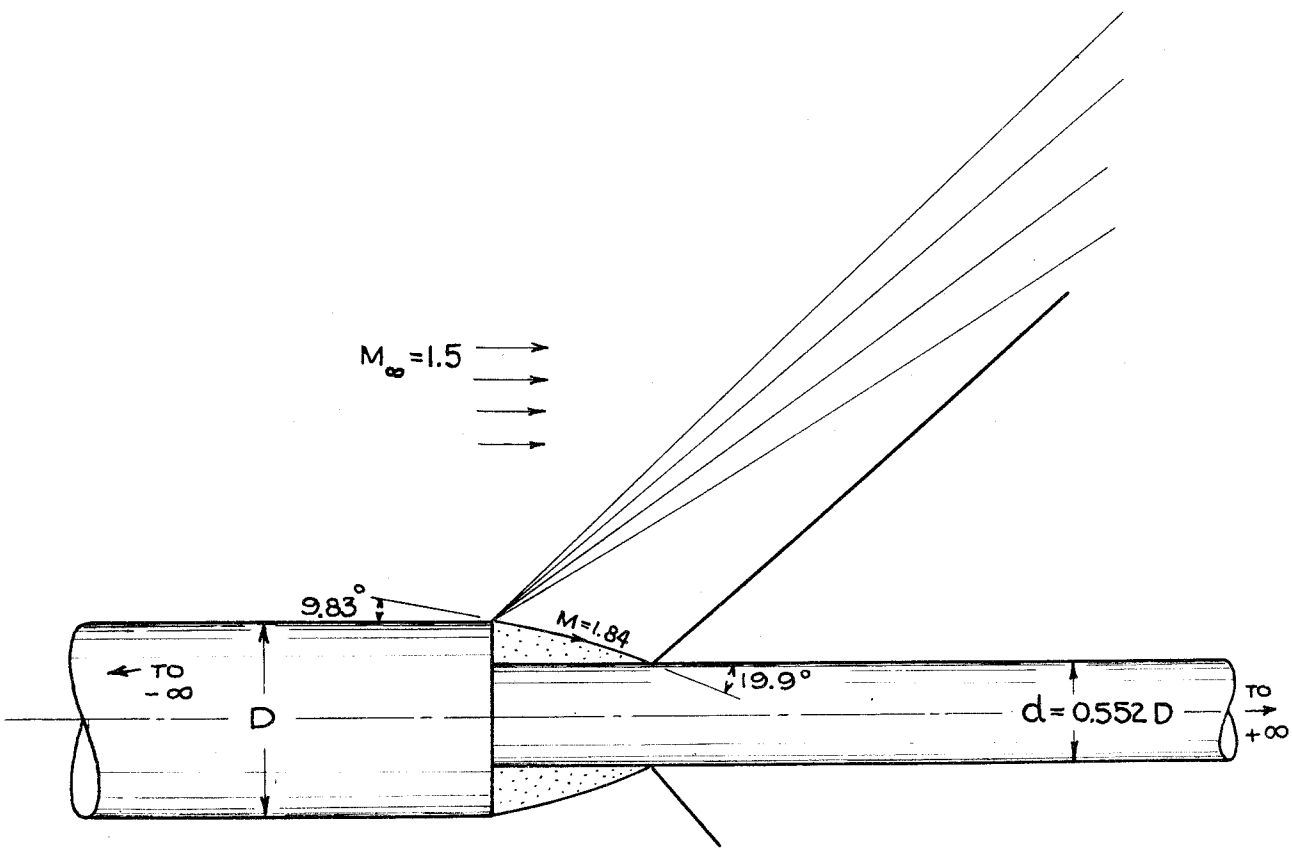

FIGURE 6:- AXIALLY-SYMMETRIC SEMI-INFINITE BODY WITH ROD ATTACHED.

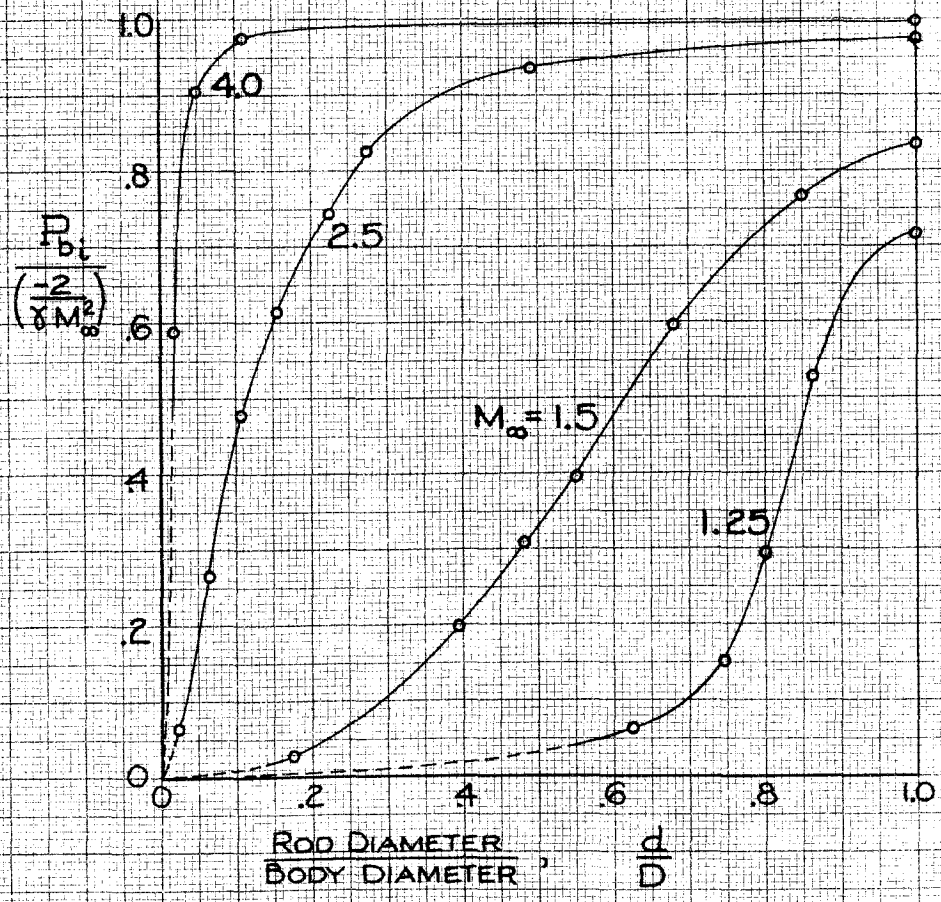

FIGURE 7:- MAXIMUM BASE DRAG POSSIBLE IN AN INVISCID AXIALLY-SYMMETRIC FLOW

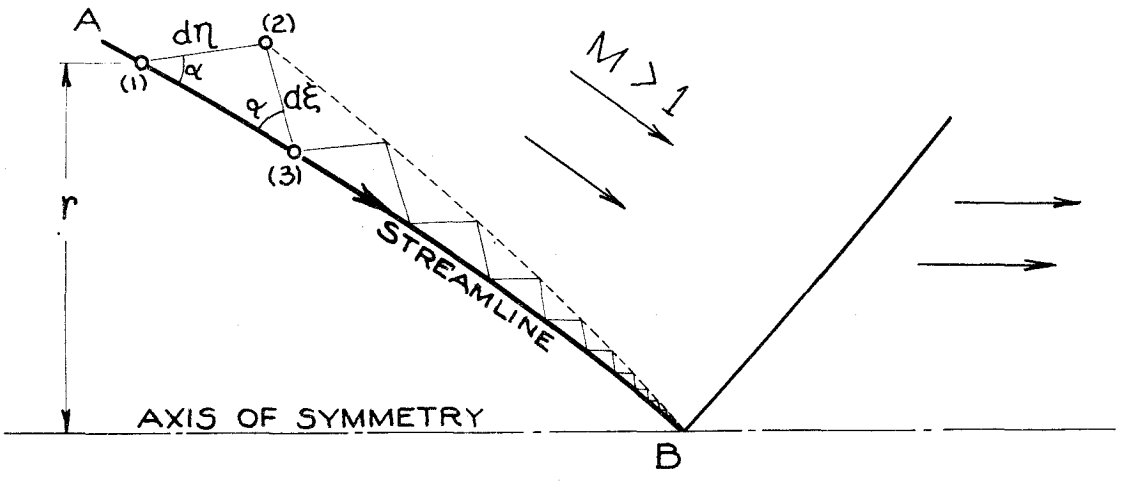

FIGURE 8a:- ASSUMED FLOW IN THE PHYSICAL PLANE

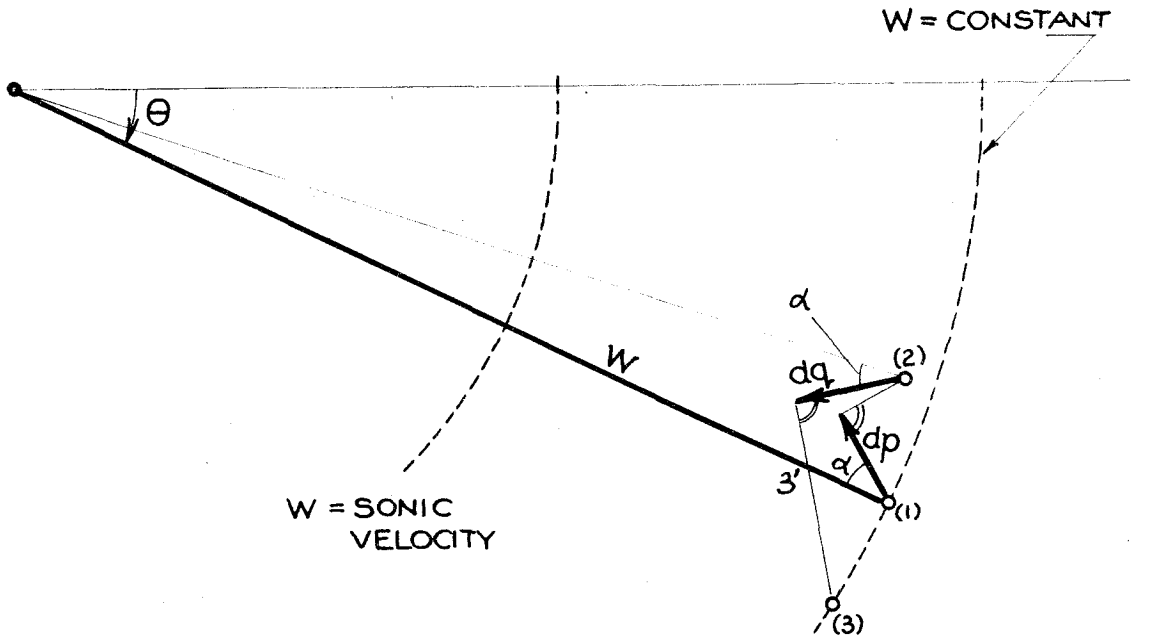

FIGURE 8b:- INCREMENTS IN HODOGRAPH PLANE CORRESPONDING TO FIGURE 8a.

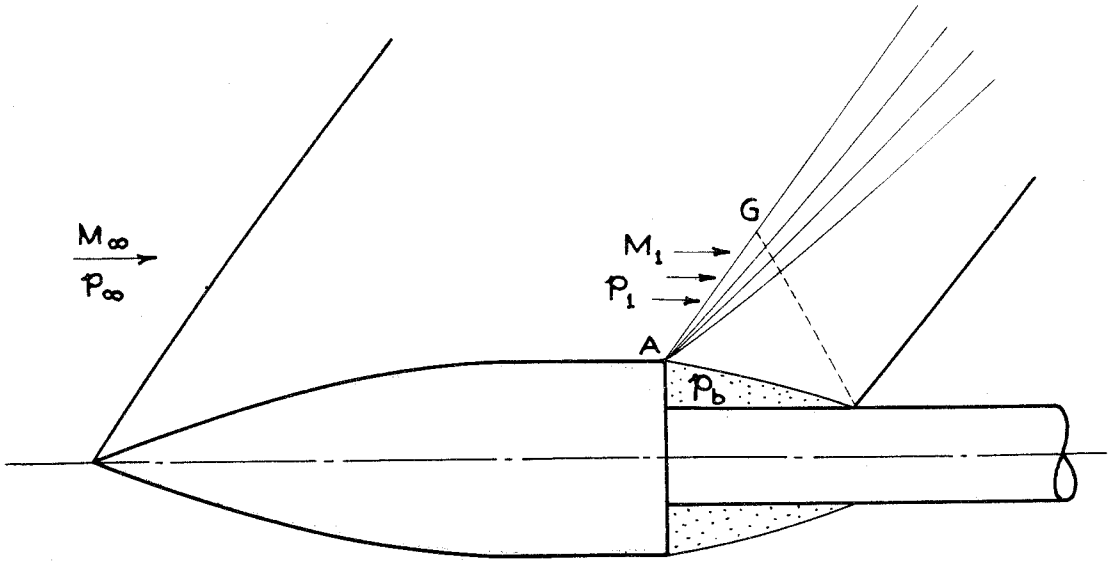

FIGURE 9a:- FINITE AXIALLY-SYMMETRIC BODY WITH ROD ATTACHED; INVISCID FLOW.

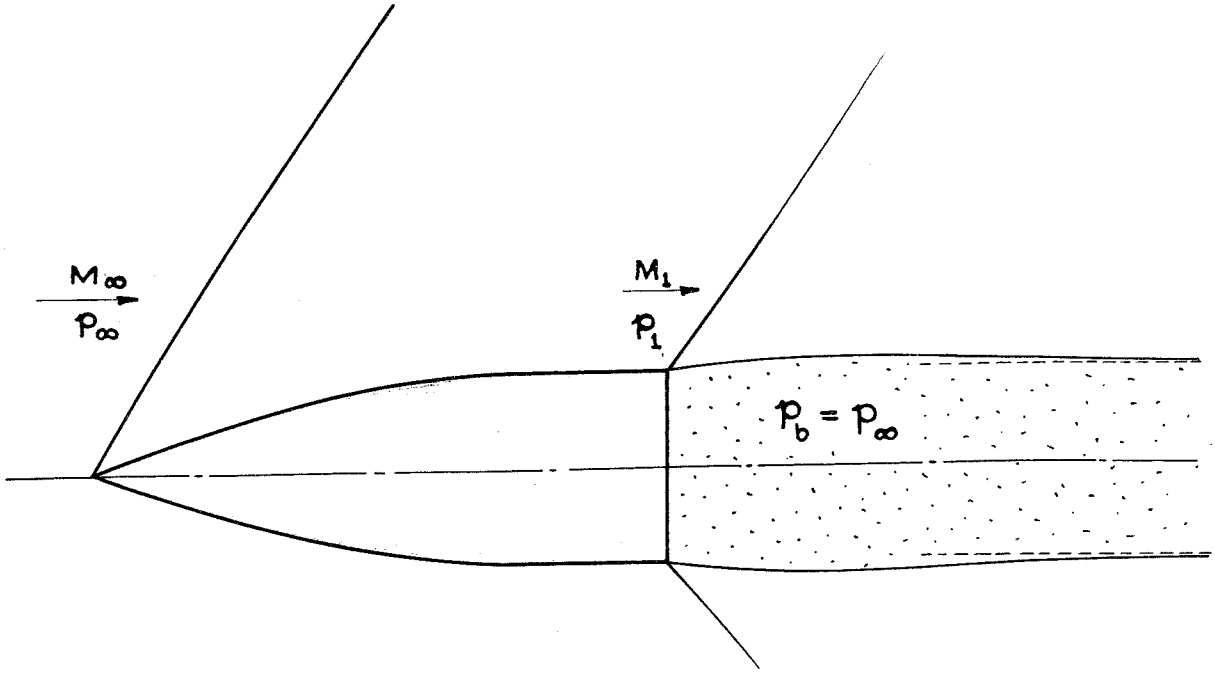

FIGURE 9b:- FINITE AXIALLY-SYMMETRIC BODY; INVISCID FLOW.

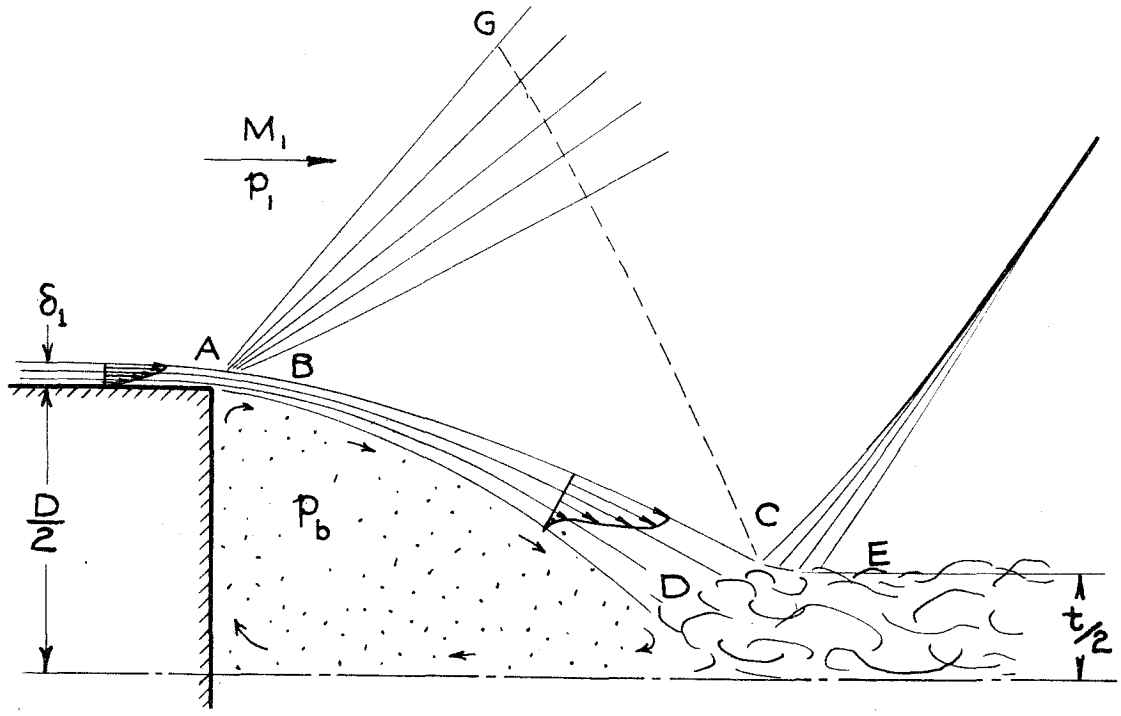

FIGURE 10:- SKETCH OF THE VISCOUS-FLUID FLOW IN THE NEIGHBORHOOD OF THE BASE

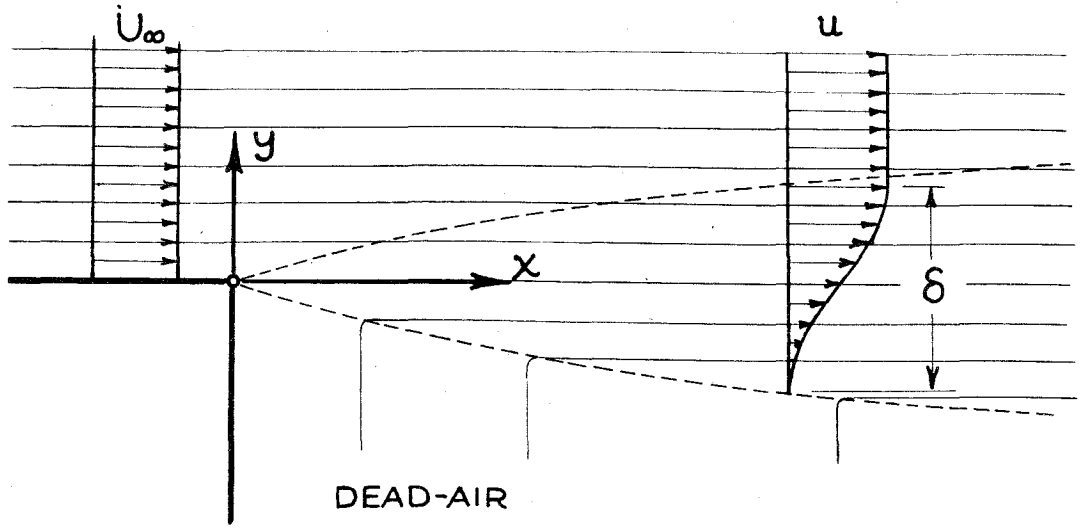

FIGURE 11:- MIXING OF STREAM WITH DEAD-AIR

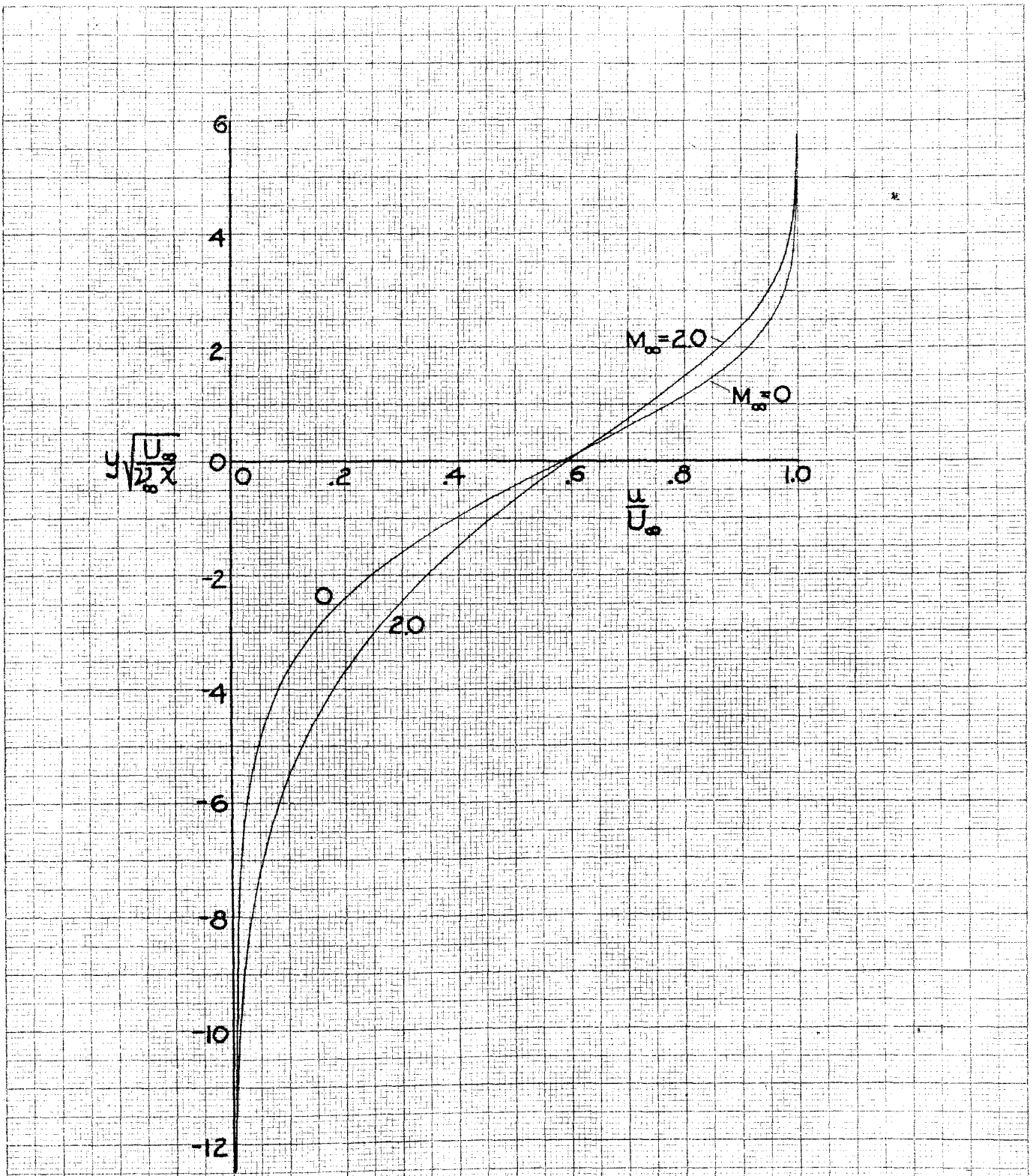

FIGURE 12:- VELOCITY PROFILES FOR LAMINAR MIXING OF A STREAM WITH DEAD-AIR.

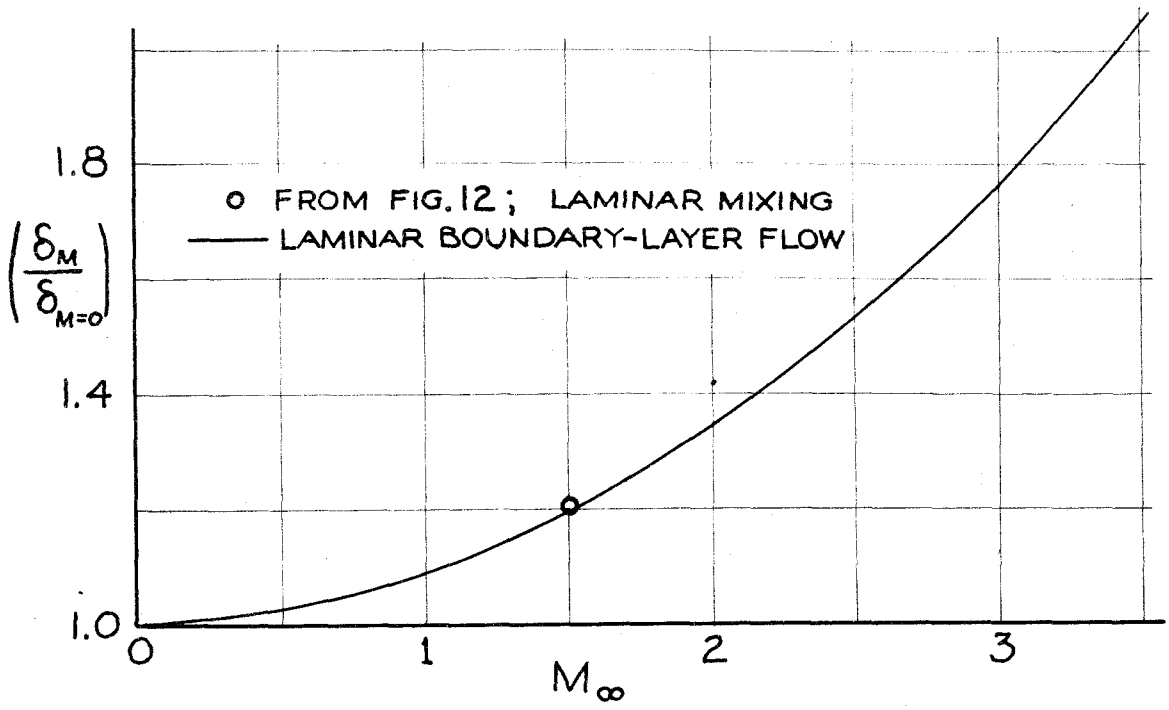

FIGURE 13:- MACH NUMBER EFFECT ON THICKNESS OF LAMINAR MIXING LAYER AND LAMINAR BOUNDARY LAYER.

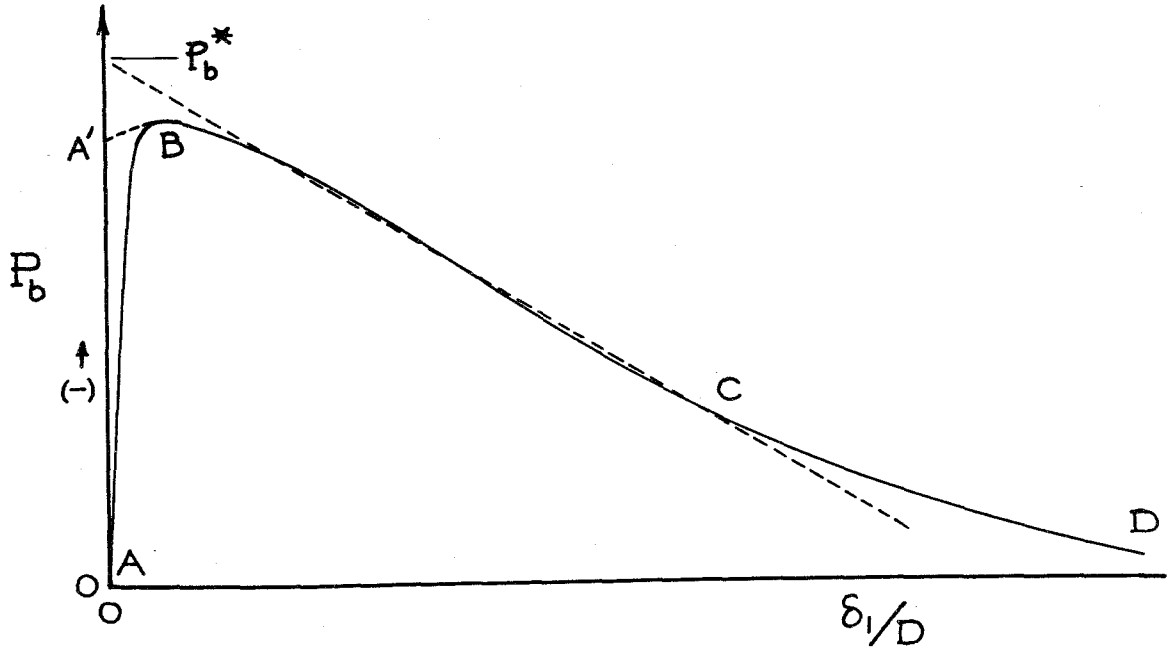

FIGURE 14:- QUALITATIVE EFFECT OF BOUNDARY-LAYER THICKNESS ON BASE PRESSURE.

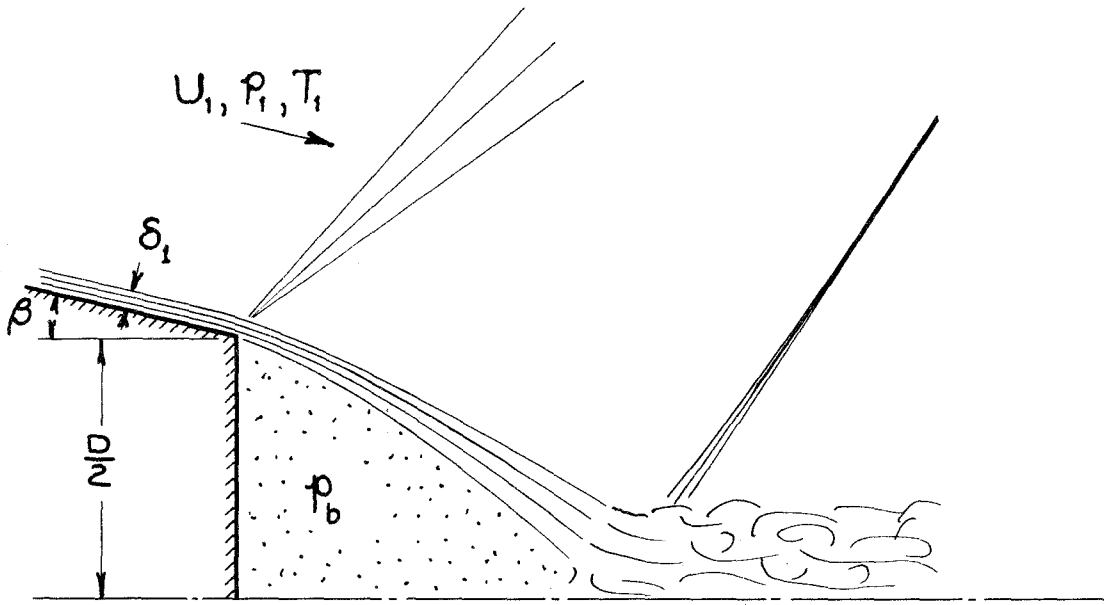

FIGURE 15:- VARIABLES AFFECTING BASE PRESSURE

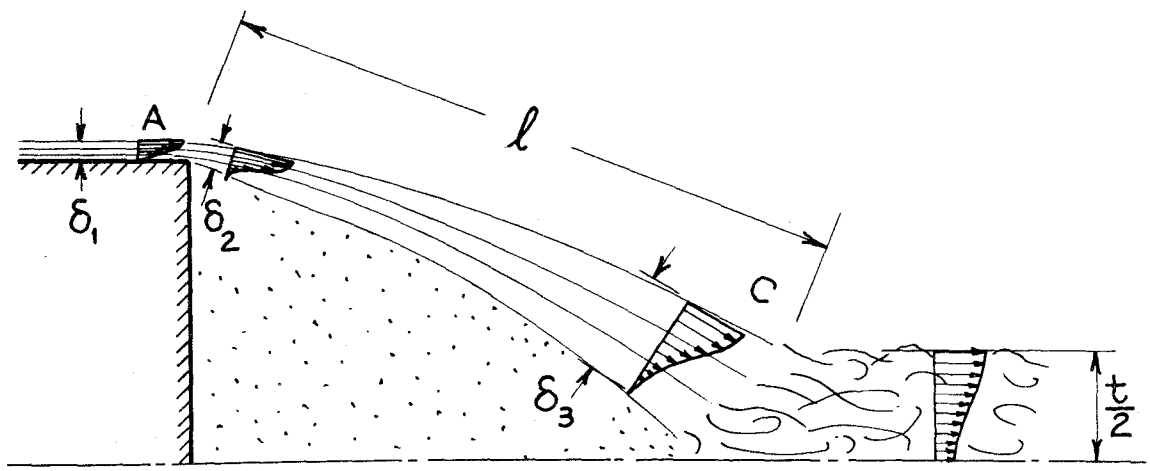

FIGURE 16:- VELOCITY PROFILES IN BOUNDARY LAYER AND IN WAKE.

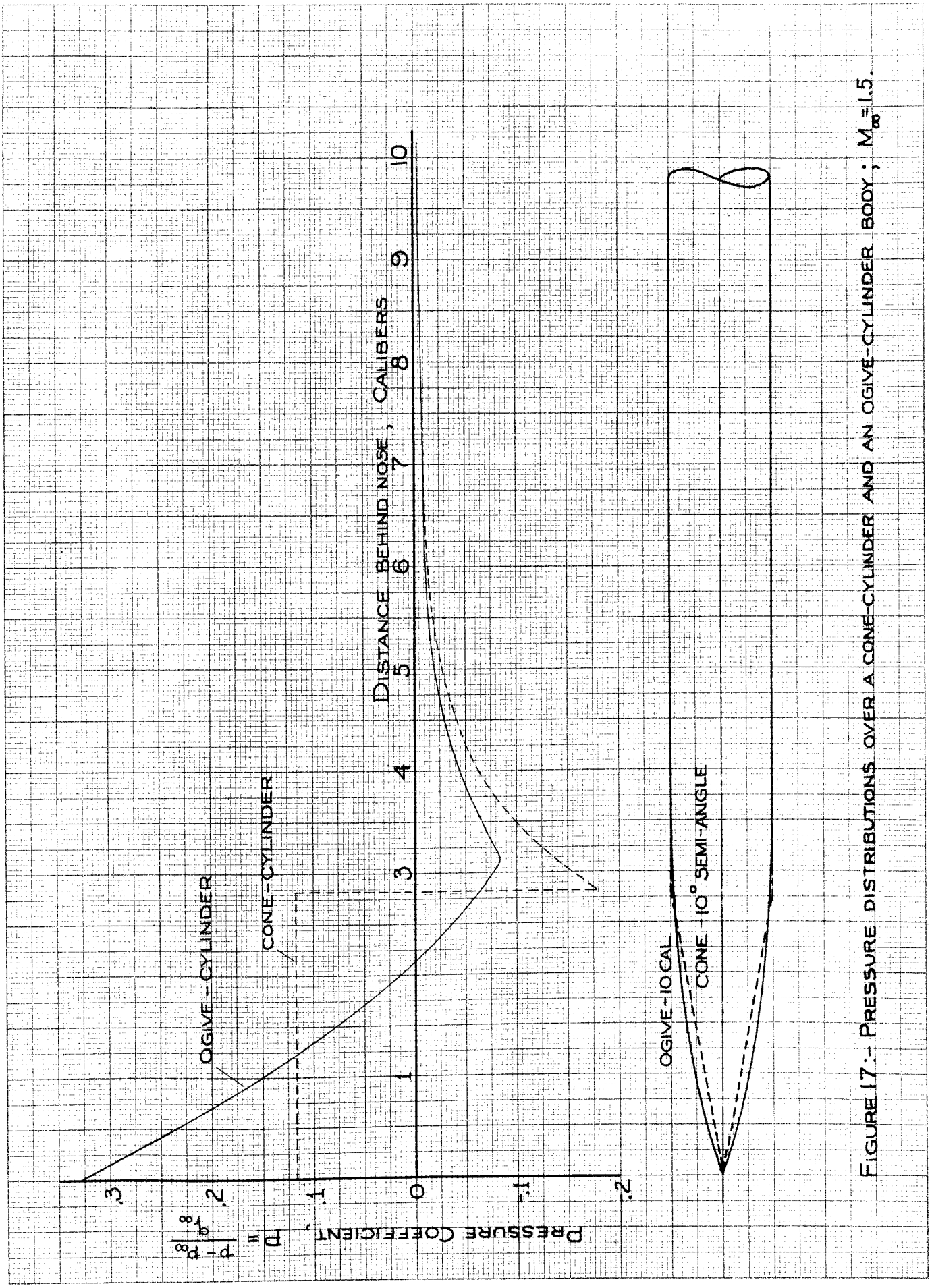

FIGURE 17:- PRESSURE DISTRIBUTIONS OVER A CONE-CYLINDER AND AN OGIVE-CYLINDER BODY; $M_\infty = 1.5$.

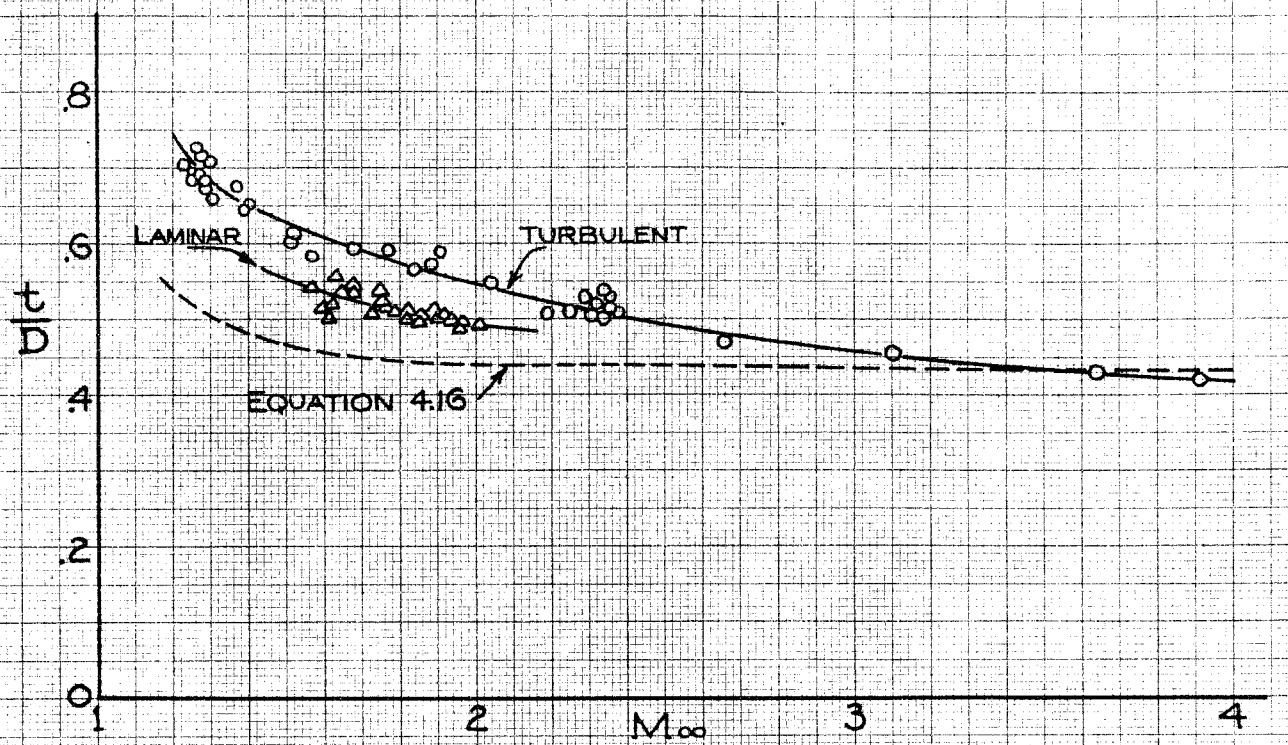

FIGURE 20:- WAKE THICKNESS AS A FUNCTION OF MACH NUMBER. (POINTS TAKEN FROM SHADOW-PHOTOGRAPHS OF THE BALLISTIC RESEARCH LABORATORIES, ABERDEEN, MD.)

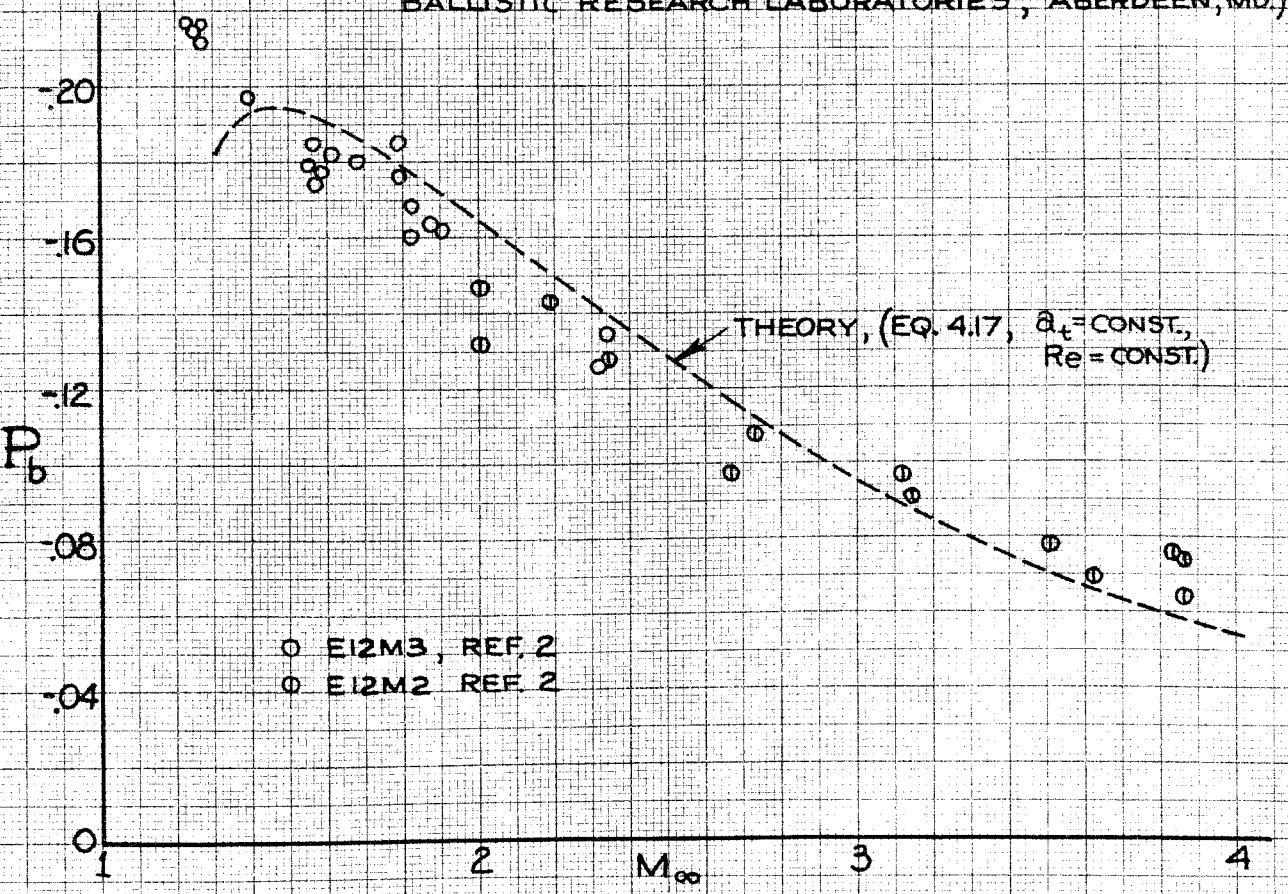

FIGURE 21:- BASE PRESSURE COEFFICIENT AS A FUNCTION OF MACH NUMBER.

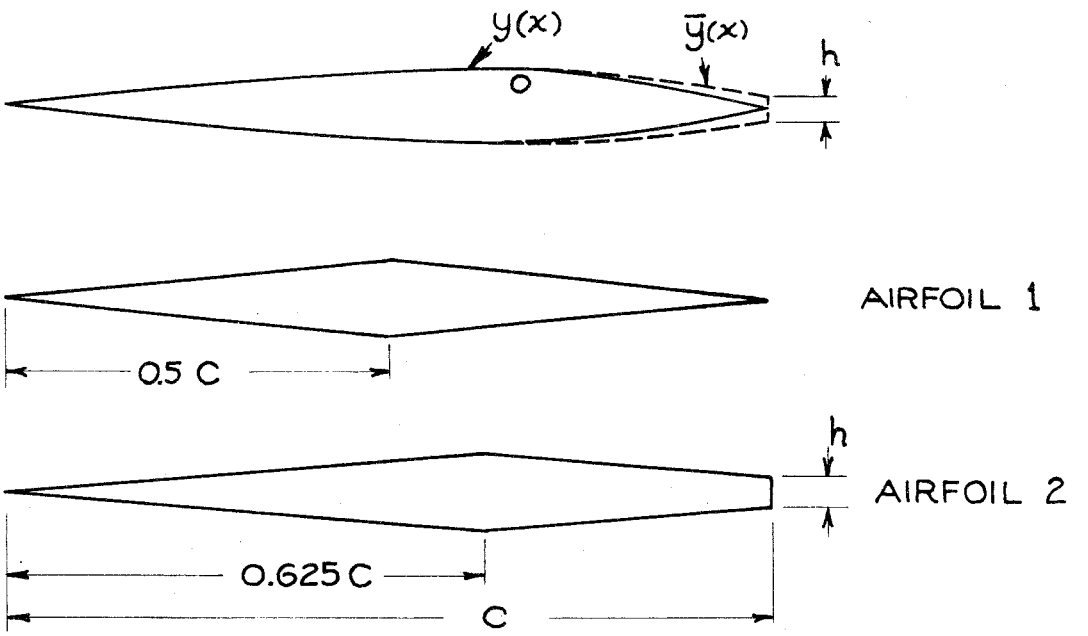

FIGURE 22 :- AIRFOIL SHAPES

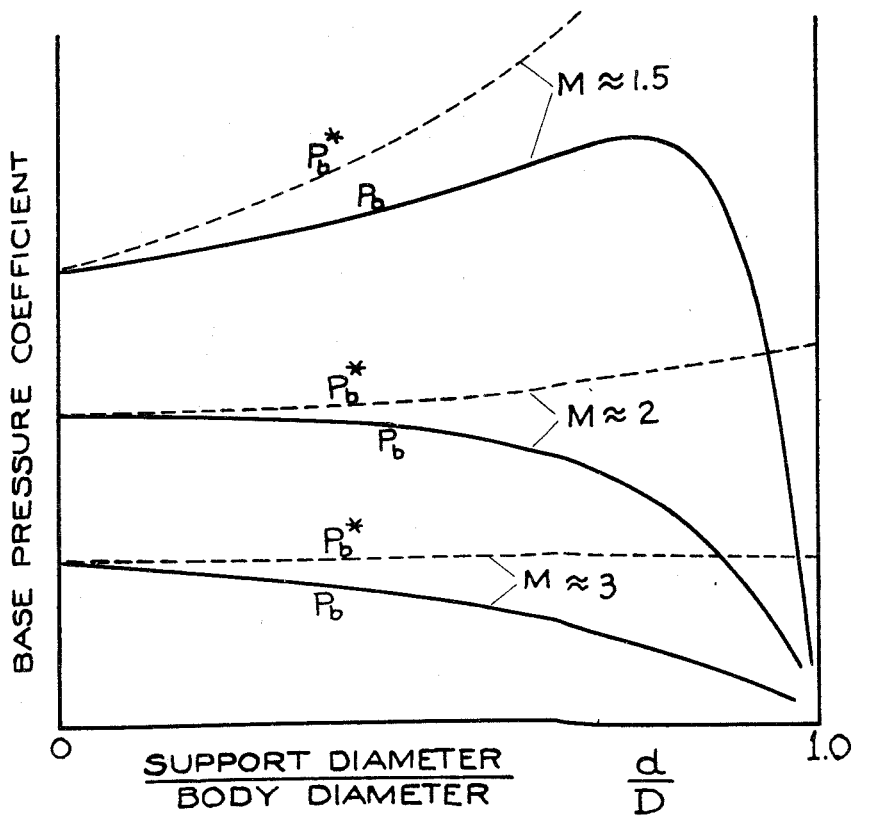

FIGURE 23 :- EFFECT OF SUPPORT DIAMETER ON BASE PRESSURE COEFFICIENT

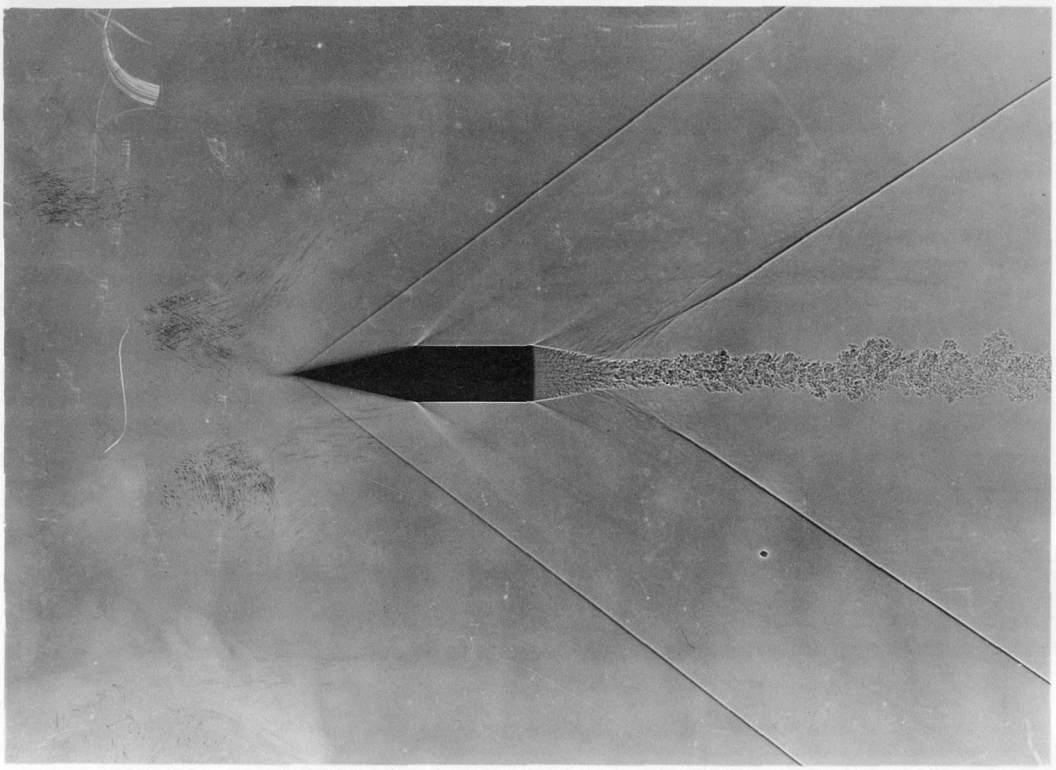

(a) $M_\infty = 1.68$, LAMINAR

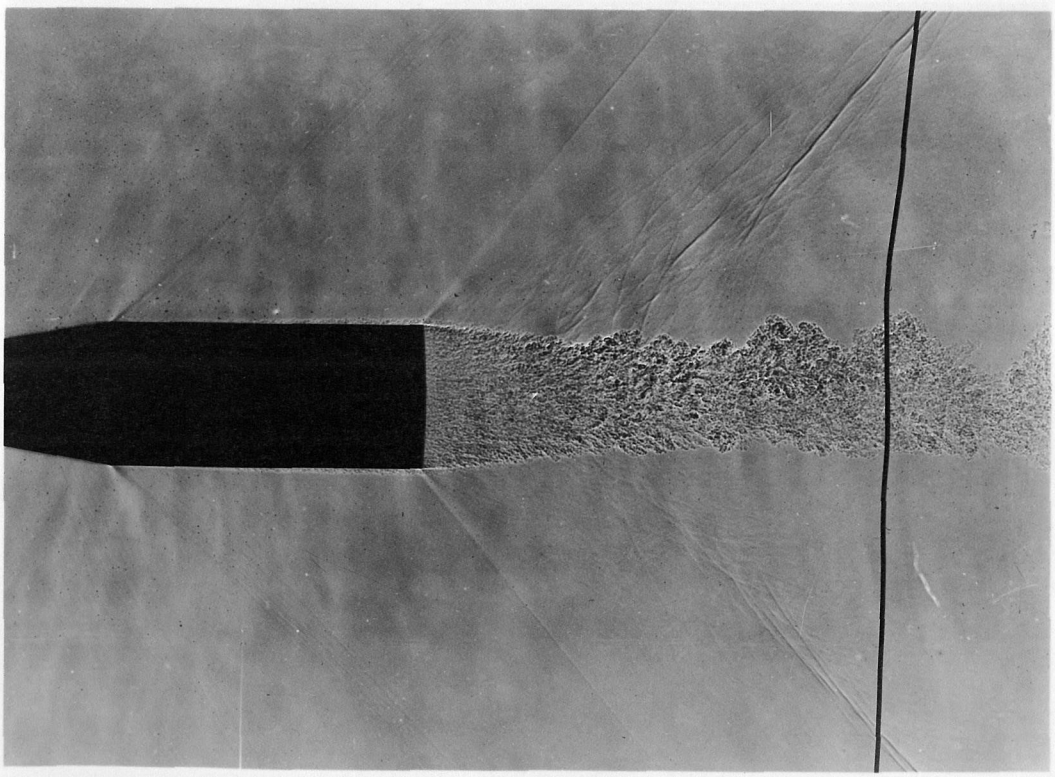

(b) $M_\infty = 1.28$, TURBULENT

FIGURE 24:- SHADOWGRAPHS OF PROJECTILES IN FLIGHT. (COURTESY BALLISTIC RESEARCH LABORATORIES, ABERDEEN, MD.)

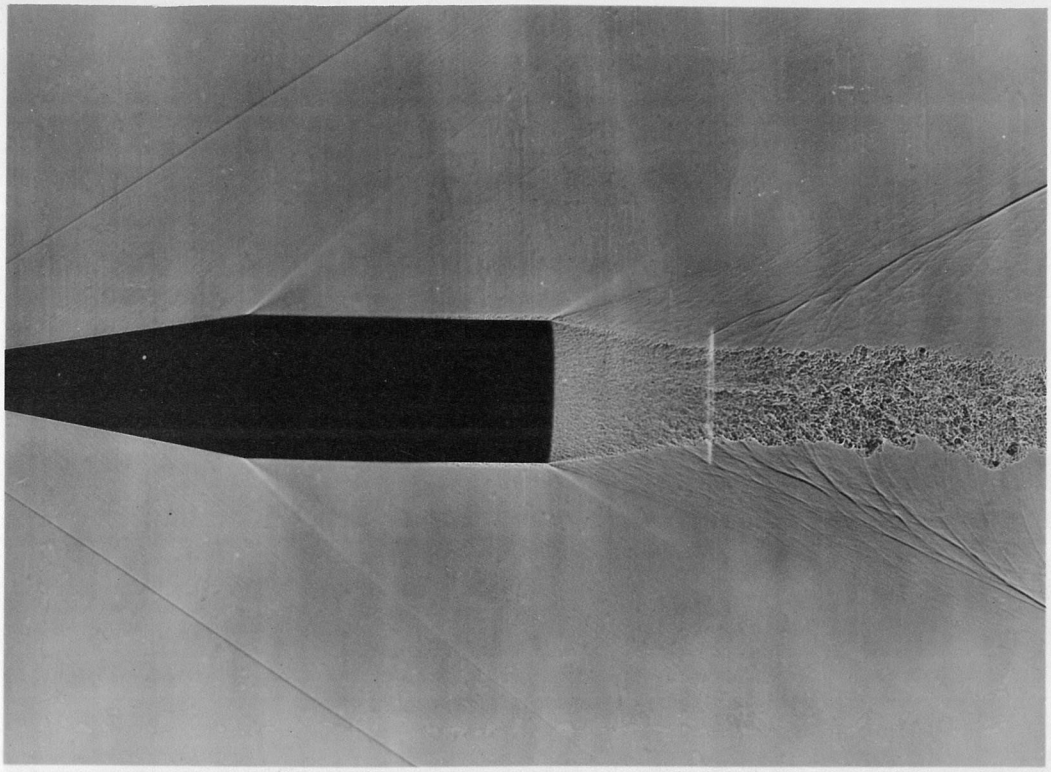

(c) $M_\infty = 1.88$, TURBULENT

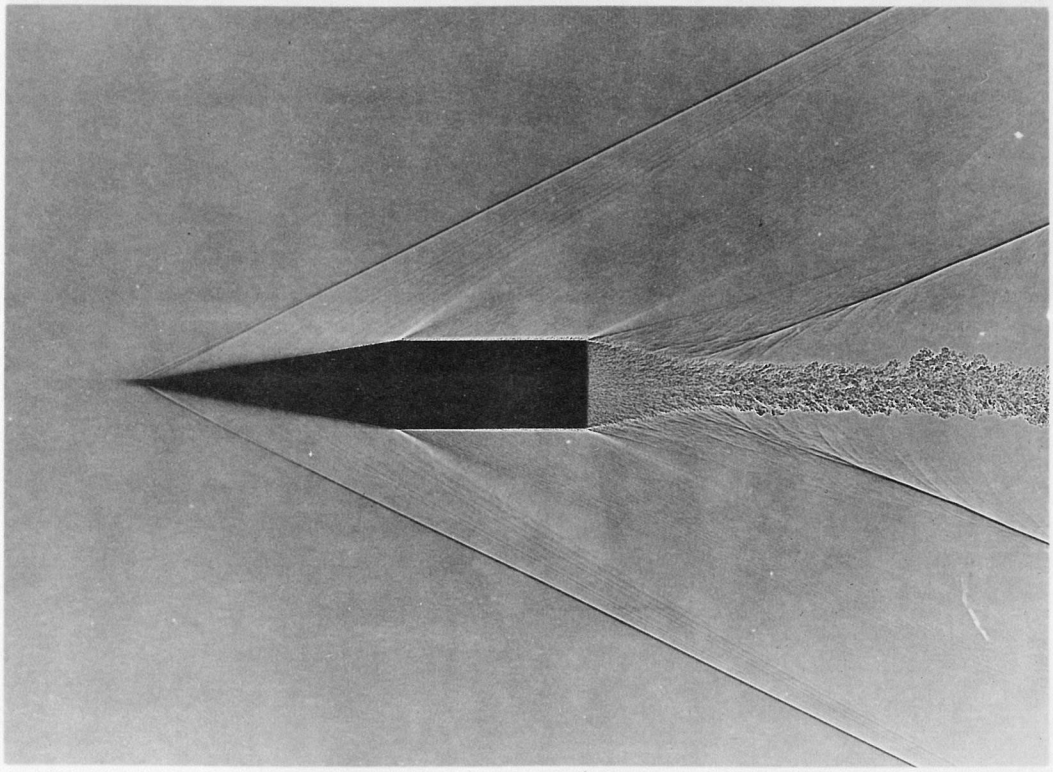

(d) $M_\infty = 2.33$ TURBULENT

FIGURE 24:- CONTINUED

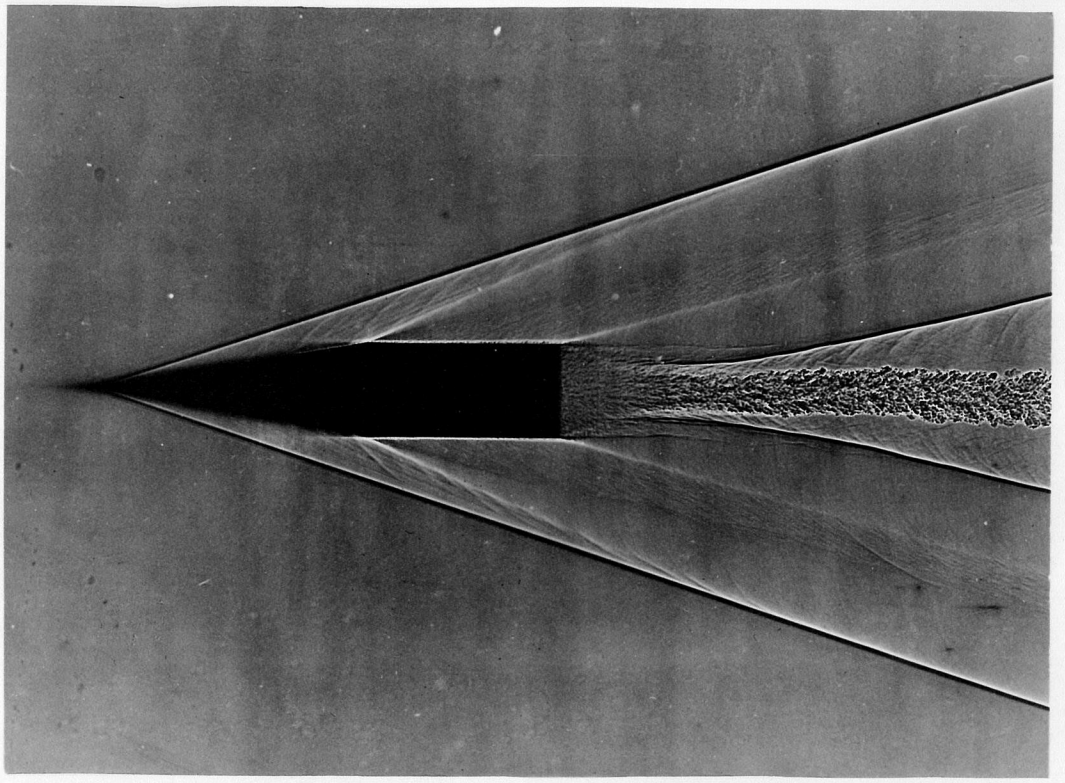

(e) M_∞=3.64, TURBULENT

FIGURE 24:- CONCLUDED